Microscopic description for polarization in particle scattering

Jun-jie Zhang,[1] Ren-hong Fang,[2] Qun Wang,[1] and Xin-Nian Wang[2,3]

[1]Department of Modern Physics, University of Science and Technology of China, Hefei, Anhui 230026, China

[2]Key Laboratory of Quark and Lepton Physics (MOE) and Institute of Particle Physics, Central China Normal University, Wuhan, Hubei 430079, China

[3]Nuclear Science Division, MS 70R0319, Lawrence Berkeley National Laboratory, Berkeley, California 94720, USA

(Received 25 April 2019; published 6 December 2019)

We propose a microscopic description for the polarization from the first principle through the spin-orbit coupling in particle collisions. It is based on scatterings of particles as wave packets, an effective method to deal with particle scatterings at specified impact parameters. The polarization is then the consequence of particle collisions in a nonequilibrium state of spins. The spin-vorticity coupling naturally emerges from the spin orbit one encoded in polarized scattering amplitudes of collisional integrals when one assumes local equilibrium in momentum but not in spin.

DOI: 10.1103/PhysRevC.100.064904

I. INTRODUCTION

A very large orbital angular momentum (OAM) can be created in peripheral heavy ion collisions [1–7]. Such a huge OAM can be transferred to the hot and dense matter produced in collisions and make particles with spins polarized along the direction of the OAM [1,6–8]. Recently the STAR collaboration has measured the global polarization of Λ and $\bar{\Lambda}$ for the first time in Au+Au collisions at $\sqrt{s_{NN}} = 7.7$–200 GeV [9–11]. The global polarization is the net polarization of local ones in an event which is aligned in the direction of the event plane. The results show that the magnitude of the global Λ and $\bar{\Lambda}$ polarization is of the order a few percent and decreases with collisional energies. The difference between the global polarization of Λ and $\bar{\Lambda}$ may possibly indicate the effect from the strong magnetic field formed in high energy heavy ion collisions.

Several theoretical models have been developed to study the global polarization. If the spin degree of freedom is thermalized, one can construct the statistic-hydro model by including the spin-vorticity coupling $S_{\mu\nu}\omega^{\mu\nu}$ into the thermal distribution function [12–14]. Here $S_{\mu\nu}$ is the spin tensor, $\omega^{\mu\nu} = -(1/2)(\partial^\mu\beta^\nu - \partial^\nu\beta^\mu)$ is the thermal vorticity, the macroscopic analog of the local OAM, and $\beta^\mu \equiv \beta u^\mu$ is the thermal velocity with $\beta = 1/T$ being the inverse of the temperature and u^μ being the fluid velocity. It turns out that the average spin or polarization is proportional to the thermal vorticity if the spin-vorticity coupling is weak. One can also derive an ideal spin hydrodynamics from the spin dependent phase space distribution functions which are 2×2 matrices [15–17]. The spin polarization tensor $\omega^{\mu\nu}$ is no longer the thermal vorticity but is treated as a set of independent hydrodynamic variables [15–17]. For a review of the spin-hydrodynamic approach, see Ref. [18].

Similar to the statistic-hydro model, another approach to the global polarization assuming local equilibrium is the Wigner function (WF) formalism. The WF formalism for spin-1/2 fermions [19–25] has recently been revived to study the chiral magnetic effect (CME) [26–29] (for reviews, see, e.g., Refs. [29–31]) and chiral vortical effect (CVE) [32–37] for massless fermions [36,38–44]. The Wigner functions for spin-1/2 fermions are 4×4 matrices. The axial vector component gives the spin phase space distribution of fermions near thermal equilibrium [45–48]. It can be shown that when the thermal vorticity is small, the spin polarization of fermions from the WF is proportional to the thermal vorticity vector. So the WF can also be applied to the study of the global polarization of hyperons.

In order to describe the STAR data on the global $\Lambda/\bar{\Lambda}$ polarization, the hydrodynamic or transport models have been used to calculate the vorticity fields in heavy ion collisions [49–55]. Then the polarization of $\Lambda/\bar{\Lambda}$ can be obtained from vorticity fields at the freezeout when the $\Lambda/\bar{\Lambda}$ hyperons are decoupled from the rest of the hot and dense matter [56–59].

Most of these models are based on the assumption that the spin degree of freedom has reached local equilibrium. But this assumption is not justified. The recent disagreement between some theoretical models and data on the longitudinal polarization indicates that the spins might not be in local equilibrium [11,60,61], or the form of the spin-vorticity coupling in local equilibrium might be different from that in global equilibrium [62,63], or any other mechanisms. Although one model of the chiral kinetic theory can explain the sign of the data [64], it is based on massless fermions and cannot reproduce the magnitude of the data. To clarify the above situations, one needs to answer the question: how is the polarization generated in microscopic collision processes? This is related to the role of the spin-orbit coupling which is regarded as the microscopic mechanism for the global polarization. The need for particle collision processes is also supported by an observation in the Lagrangian formulation of relativistic hydrodynamics for spin fluids: the ideal limit of hydrodynamics with spin is generally acausal [65], hence nonequilibrium spin degrees of freedom are necessary. In one particle scattering such as a 2-to-2 scattering at fixed impact parameter the effect of spin-orbit coupling in the polarized cross section is obvious [1,6], but how does the spin-vorticity coupling naturally emerge from the spin-orbit one? It is far from easy and obvious as it involves the treatment of particle scatterings at different space-time points in a system of particles in randomly distributed momentum. To the best of our knowledge, this problem has not been seriously investigated due to such a difficulty. In this paper we will construct a microscopic model for the global polarization based on the spin-orbit coupling. We will show that the spin-vorticity coupling naturally emerges from scatterings of particles at different space-time points incorporating polarized scattering amplitudes with the spin-orbit coupling. This provides a microscopic mechanism for the global polarization from the first principle through particle collisions in nonequilibrium.

The paper is organized as follows. In Sec. II we will introduce scatterings of two wave packets for spin-0 particles. The wave packet method is necessary to describe particle scatterings at different space-time points. In Sec. III we will study collisions of spin-0 particles as wave packets which take place at different space-time in a multiparticle system. In Sec. IV we will derive the polarization rate for spin-1/2 particles from particle collisions. As an example, we will apply in Sec. V the formalism to derive the quark polarization rate in a quark-gluon plasma in local equilibrium in momentum. In Sec. VI we will discuss the numerical method to calculate the quark polarization rate, a challenging task to deal with collision integrals in very high dimensions. We will present the numerical results in Sec. VII. Finally we will give a summary of the work and an outlook for future studies.

Throughout the paper we use natural units $\hbar = c = k_B = 1$. The convention for the metric tensor is $g^{\mu\nu} = \text{diag}(+1, -1, -1, -1)$. We also use the notation $a^\mu b_\mu \equiv a \cdot b$ for the scalar product of two four-vectors a^μ, b^μ and $\mathbf{a} \cdot \mathbf{b}$ for the corresponding scalar product of two spatial vectors $\mathbf{a}$, $\mathbf{b}$. The direction of a three-vector $\mathbf{a}$ is denoted as $\hat{\mathbf{a}}$. Sometimes we denote the components of a three-vector by indices (1,2,3) or (x, y, z).

II. SCATTERINGS OF WAVE PACKETS FOR SPIN-0 PARTICLES

In this section we will consider the scattering process $A + B \to 1 + 2 \cdots + n$, where the incident particles A and B in the remote past are localized in some region and can be described by wave packets. The details of this section can be found in the textbook by Peskin and Schroeder [66]. The purpose of this section is to give an idea of how the wave packets displaced by an impact parameter are treated in the scattering process, and to provide the basis for the discussion in the next section. We work in the frame in which the central momenta of two wave packets are collinear or in the same direction which we denote as the longitudinal direction. We assume that the wave packet B is displaced by an impact parameter vector $\mathbf{b}$ in the transverse direction, so the *in* state can be written as

$$|\phi_A\phi_B\rangle_{\text{in}} = \int \frac{d^3k_A}{(2\pi)^3}\frac{d^3k_B}{(2\pi)^3}\frac{\phi_A(\mathbf{k}_A)\phi_B(\mathbf{k}_B)e^{-i\mathbf{k}_B\cdot\mathbf{b}}}{\sqrt{4E_AE_B}}|\mathbf{k}_A\mathbf{k}_B\rangle_{\text{in}}. \tag{1}$$

Here we see that the incident particles are treated as two wave packets $|\phi_A\rangle$ and $|\phi_B\rangle$ defined in Appendix A. The definition of the single particle states $|\mathbf{k}_A\rangle$ and $|\mathbf{k}_B\rangle$ can also be found in Appendix A. As we have mentioned, the amplitudes $\phi_i(\mathbf{k}_i)$ center at $\mathbf{p}_i = (0, 0, p_{iz})$ for $i = A, B$. We assume that the *out* state is a pure momentum state $|\mathbf{p}_1\mathbf{p}_2 \ldots \mathbf{p}_n\rangle_{\text{out}}$ in the far future. This is physically reasonable as long as the detectors of final-state particles mainly measure momentum or they do not resolve positions at the level of de Broglie wavelengths. Taking into account the normalization factors for the in state and out state, the scattering probability is given by

$$\begin{aligned}
&\mathcal{P}(AB \to 12\ldots n) \\
&= \sum_{\mathbf{p}_1}\sum_{\mathbf{p}_2}\cdots\sum_{\mathbf{p}_n}\frac{|_{\text{out}}\langle\mathbf{p}_1\mathbf{p}_2\ldots\mathbf{p}_n|\phi_A\phi_B\rangle_{\text{in}}|^2}{\prod_{f=1}^n\langle\mathbf{p}_f|\mathbf{p}_f\rangle\langle\phi_A|\phi_A\rangle\langle\phi_B|\phi_B\rangle} \\
&= \left(\prod_{f=1}^n\int\frac{\Omega d^3p_f}{(2\pi)^3}\right)\frac{|_{\text{out}}\langle\mathbf{p}_1\mathbf{p}_2\ldots\mathbf{p}_n|\phi_A\phi_B\rangle_{\text{in}}|^2}{\prod_{f=1}^n(2E_f\Omega)} \\
&= \left(\prod_{f=1}^n\int\frac{d^3p_f}{(2\pi)^3 2E_f}\right)|_{\text{out}}\langle\mathbf{p}_1\mathbf{p}_2\ldots\mathbf{p}_n|\phi_A\phi_B\rangle_{\text{in}}|^2,
\end{aligned} \tag{2}$$

where the normalization of single particle states and wave packets is given in Appendix A. Since $\mathcal{P}(AB \to 12\ldots n)$ depends on the impact parameter $\mathbf{b}$, we can rewrite it as $\mathcal{P}(\mathbf{b})$. This probability gives the differential cross section at the impact parameter $\mathbf{b}$,

$$\frac{d\sigma}{d^2b} = \mathcal{P}(\mathbf{b}). \tag{3}$$

The total cross section is then an integral over the impact parameter,

$$\begin{aligned}
\sigma = \int d^2b\mathcal{P}(\mathbf{b}) = &\left(\prod_{f=1}^n\int\frac{d^3p_f}{(2\pi)^3 2E_f}\right)\prod_{i=A,B}\int\frac{d^3k_i}{(2\pi)^3}\frac{\phi_i(\mathbf{k}_i)}{\sqrt{2E_i}}\int\frac{d^3k'_i}{(2\pi)^3}\frac{\phi_i^*(\mathbf{k}'_i)}{\sqrt{2E'_i}} \\
&\times\int d^2b e^{i(\mathbf{k}'_B-\mathbf{k}_B)\cdot\mathbf{b}}({}_{\text{out}}\langle\{\mathbf{p}_f\}|\{\mathbf{k}_i\}\rangle_{\text{in}})({}_{\text{out}}\langle\{\mathbf{p}_f\}|\{\mathbf{k}'_i\}\rangle_{\text{in}})^*
\end{aligned}$$

$$= \left(\prod_{f=1}^{n}\int \frac{d^3p_f}{(2\pi)^3 2E_f}\right)\left(\prod_{i=A,B}\int \frac{d^3k_i}{(2\pi)^3}\frac{\phi_i(\mathbf{k}_i)}{\sqrt{2E_{ki}}}\int \frac{d^3k_i'}{(2\pi)^3}\frac{\phi_i^*(\mathbf{k}_i')}{\sqrt{2E_{ki}'}}\right)(2\pi)^2\delta^{(2)}(\mathbf{k}_{B,\perp}'-\mathbf{k}_{B,\perp})$$
$$\times (2\pi)^4\delta^{(4)}\left(k_A'+k_B'-\sum_{f=1}^{n}p_f\right)(2\pi)^4\delta^{(4)}\left(k_A+k_B-\sum_{f=1}^{n}p_f\right)$$
$$\times\mathcal{M}(\{k_A,k_B\}\to\{p_1,p_2,\dots,p_n\})\mathcal{M}^*(\{k_A',k_B'\}\to\{p_1,p_2,\dots,p_n\}), \tag{4}$$

where $E_{ki}=\sqrt{|\mathbf{k}_i|^2+m_i^2}$, $E_{ki}'=\sqrt{|\mathbf{k}_i'|^2+m_i^2}$ with $i=A,B$, $\mathbf{k}_{B,\perp}$ denotes the transverse part of the momentum and $\mathcal{M}$ denotes the invariant amplitude of the scattering process. We can integrate out six delta functions involving $\mathbf{k}_A'$ and $\mathbf{k}_B'$, i.e., $\delta^{(2)}(\mathbf{k}_{B,\perp}'-\mathbf{k}_{B,\perp})$ and $\delta^{(4)}(k_A'+k_B'-\sum_{f=1}^{n}p_f)$. By integrating over $\mathbf{k}_{B,\perp}'$ to remove $\delta^{(2)}(\mathbf{k}_{B,\perp}'-\mathbf{k}_{B,\perp})$, we can replace $\mathbf{k}_{B,\perp}'$ by $\mathbf{k}_{B,\perp}$ in the integrand. By integrating over $\mathbf{k}_{A,\perp}'$ to remove $\delta^{(2)}(\mathbf{k}_{A,\perp}'+\mathbf{k}_{B,\perp}'-\sum_{f=1}^{n}\mathbf{p}_{f,\perp})$, we can replace $\mathbf{k}_{A,\perp}'$ by $-\mathbf{k}_{B,\perp}+\sum_{f=1}^{n}\mathbf{k}_{f,\perp}$ in the integrand. Then we can integrate over $k_{B,z}'$ to remove $\delta(k_{A,z}'+k_{B,z}'-p_{1,z}-p_{2,z})$, in which $k_{B,z}'$ is replaced by $\sum_{f=1}^{n}p_{f,z}-k_{A,z}'$. The last variable that can be integrated over is $k_{A,z}'$ in the delta function for the energy conservation $\delta(E_A'+E_B'-E_{p1}-E_{p2})$. We can solve $k_{A,z}'$ as the root of the equation $E_A'+E_B'=E_{p1}+E_{p2}$. Note that E_A' and E_B' are given by

$$E_A'=\sqrt{\left(-\mathbf{k}_{B,\perp}+\sum_{f=1}^{n}\mathbf{k}_{f,\perp}\right)^2+k_{A,z}'^2+m_A^2},$$
$$E_B'=\sqrt{\mathbf{k}_{B,\perp}^2+\left(\sum_{f=1}^{n}p_{f,z}-k_{A,z}'\right)^2+m_B^2}. \tag{5}$$

The delta function can be rewritten as

$$\delta\left(E_A'+E_B'-\sum_{f=1}^{n}E_f\right)=\sum_j\left|\frac{k_{A,z,j}'}{E_A'}-\frac{k_{B,z,j}'}{E_B'}\right|^{-1}\delta(k_{A,z}'-k_{A,z,j}'), \tag{6}$$

where $k_{A,z,j}'$ are the roots of the equation $E_A'+E_B'=E_{p1}+E_{p2}$.

If we assume that the incident wave packets are narrow in momentum and centered at momenta $\mathbf{p}_A$ and $\mathbf{p}_B$, i.e., $\phi_i(\mathbf{k}_i)$ are close to delta functions $\delta(\mathbf{k}_i-\mathbf{p}_i)$, we can approximate $(E_{kA}',\mathbf{k}_A')\approx(E_{kA},\mathbf{k}_A)\approx(E_A,\mathbf{p}_A)$ and $(E_B',\mathbf{k}_B')\approx(E_{kB},\mathbf{k}_B)\approx(E_B,\mathbf{p}_B)$. We can also approximate $v_i=p_{i,z}/E_i\approx k_{i,z}'/E_i'$ with $i=A,B$. Then we obtain

$$\sigma\approx\left(\prod_{f=1}^{n}\int\frac{d^3p_f}{(2\pi)^3 2E_f}\right)\int\frac{d^3k_A}{(2\pi)^3}\frac{|\phi_A(\mathbf{k}_A)|^2}{2E_A}\int\frac{d^3k_B}{(2\pi)^3}\frac{|\phi_B(\mathbf{k}_B)|^2}{2E_B}|v_A-v_B|^{-1}(2\pi)^4\delta\left(p_A+p_B-\sum_{f=1}^{n}p_f\right)|\mathcal{M}(\{p_i\}\to\{p_f\})|^2$$
$$=\frac{1}{4E_AE_B|v_A-v_B|}\left(\prod_{f=1}^{n}\int\frac{d^3p_f}{(2\pi)^3 2E_f}\right)(2\pi)^4\delta\left(p_A+p_B-\sum_{f=1}^{n}p_f\right)|\mathcal{M}(\{p_i\}\to\{p_f\})|^2. \tag{7}$$

Here we have used the normalization condition for the wave amplitude (A9). We note that the above formula is derived in the frame in which incident particles are collinear in momentum. We can boost the frame to the center-of-mass frame of the incident particles and the cross section is invariant.

If the number densities of A and B in coordinate space are n_A and n_B respectively, the collision rate, i.e., the number of scatterings per unit time and unit volume is given by

$$R=n_An_B|v_A-v_B|\sigma=\frac{n_An_B}{4E_AE_B}4E_AE_B|v_A-v_B|\sigma, \tag{8}$$

where we have rewritten the rate in a Lorentz invariant way by making use of the fact that $4E_AE_B|v_A-v_B|$, n_A/E_A and n_B/E_B are Lorentz invariant along the collision axis.

III. COLLISION RATE FOR SPIN-0 PARTICLES IN A MULTIPARTICLE SYSTEM

In this section we will derive the collision rate in a system of spin-0 particles of multispecies. We will generalize the result of the previous section by treating the incident particles as wave packets. The emphasis is put on the collision of two particles at two different space-time points.

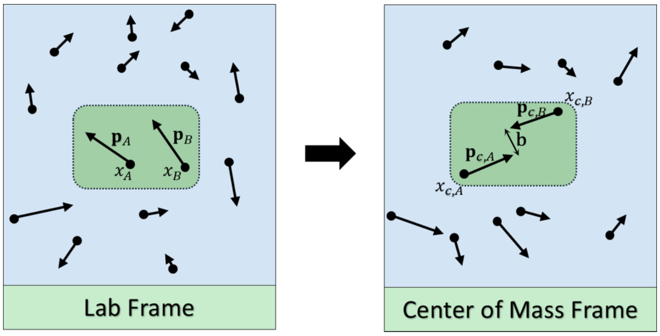

FIG. 1. A collision or scattering in the laboratory frame (left) and center-of-mass frame (right).

We will frequently use two frames in this and the next section: the laboratory frame and the center-of-mass system (CMS) of one specific collision. In the laboratory frame, the movement of one species of particles follows their phase space distribution $f(x, p)$. There are many collisions taking place in the system. Figure 1 shows one collision of two incident particles at $x_A = (t_A, \mathbf{x}_A)$ and $x_B = (t_B, \mathbf{x}_B)$ in the laboratory frame and CMS. We see that $\mathbf{p}_A$ and $\mathbf{p}_B$ are not aligned in the same direction in the laboratory frame. When boosted to the CMS of this collision with the boost velocity determined by $\mathbf{v}_{\rm bst} = (\mathbf{p}_A + \mathbf{p}_B)/(E_A + E_B)$, we have $\mathbf{p}_{c,A} + \mathbf{p}_{c,B} = 0$ as shown in the right panel of Fig. 1; see Appendix C for more details of such a Lorentz transformation. Hereafter we denote the quantities in the CMS by the index c. There is an inherent problem in the collision of incident particles located at different space-time points: the collision time is not well defined. If we assume that the collision takes place at the same time in the laboratory frame, i.e., $t_A = t_B$, after being boosted to the CMS, the time will be mismatched, i.e., $t_{c,A} \neq t_{c,B}$, since $\mathbf{x}_A$ and $\mathbf{x}_B$ are different. The reverse statement is also true: if $t_{c,A} = t_{c,B}$ then $t_A \neq t_B$ due to $\mathbf{x}_{c,A} \neq \mathbf{x}_{c,B}$. Such an ambiguity in the collision time cannot be avoided but can be constrained by the requirement that the difference $\Delta t_c = t_{c,A} - t_{c,B}$ should not be large, otherwise the incident particles are irrelevant or the collision is uncausal in the CMS. In the calculation of this paper, we will put a simple constraint $\Delta t_c = 0$. In the right panel of Fig. 1, we also see that the impact parameter $\mathbf{b}$ is given by the distance of $\mathbf{x}_{c,A}$ and $\mathbf{x}_{c,B}$ in the transverse direction which is perpendicular to $\mathbf{p}_{c,A}$ or $\mathbf{p}_{c,B}$. In the longitudinal direction or the direction of $\mathbf{p}_{c,A}$ or $\mathbf{p}_{c,B}$, two space points are also different in general, i.e., $\hat{\mathbf{p}}_{c,A} \cdot \mathbf{x}_{c,A} \neq \hat{\mathbf{p}}_{c,A} \cdot \mathbf{x}_{c,B}$. In the calculation we also require that the distance between two space points in the longitudinal direction, $\Delta x_{c,L} = \hat{\mathbf{p}}_{c,A} \cdot (\mathbf{x}_{c,A} - \mathbf{x}_{c,B})$, should not be large, otherwise the incident particles as wave packets lose coherence and cannot interact in the CMS. In the calculation, we will also put a simple constraint $\Delta x_{c,L} = 0$. The CMS constraint $\Delta t_c = 0$ and $\Delta x_{c,L} = 0$ is equivalent to the condition $\Delta t = \mathbf{v}_{\rm bst} \cdot \Delta \mathbf{x}$ and $(\mathbf{v}_A - \mathbf{v}_B) \cdot \Delta \mathbf{x} = 0$ in the laboratory frame; see Appendix C for the derivation.

Since we will work in the CMS of incident particles in each collision, for notational simplicity, we will suppress the index c (standing for the CMS) of all quantities in the rest part of this section. So all quantities are implied in the CMS if not explicitly stated here.

We know that the momentum integral of the distribution function gives the number density in the coordinate space. Similar to Eq. (8), the collision rate in corresponding momentum and space-time intervals can be written as

$$R_{AB\to 12} = \frac{d^3 p_A}{(2\pi)^3} \frac{d^3 p_B}{(2\pi)^3} f_A(x_A, p_A) f_B(x_B, p_B) |v_A - v_B| \Delta\sigma, \tag{9}$$

where $v_A = |\mathbf{p}_A|/E_A$ and $v_B = -|\mathbf{p}_B|/E_B$ are the longitudinal velocities with $\mathbf{p}_A = -\mathbf{p}_B$ in the CMS, f_A and f_B are the phase space distributions for the incident particle A and B respectively, and $\Delta\sigma$ denotes the infinitesimal element of the cross section given by

$$\Delta\sigma = \frac{1}{C_{AB}} d^4x_A d^4x_B \delta(\Delta t)\delta(\Delta x_L) \times \frac{d^3p_1}{(2\pi)^3 2E_1} \frac{d^3p_2}{(2\pi)^3 2E_2} \frac{1}{(2E_A)(2E_B)} K. \tag{10}$$

Here we have assumed that the scattering takes place at the same time and the same longitudinal position in the CMS, so we put two delta functions to implement these constraints. The constant C_{AB} is to make $\Delta\sigma$ have the right dimension of the cross section and will be defined later. In Eq. (10) K is given by

$$\begin{aligned} K &= (2E_A)(2E_B) |{}_{\rm out}\langle p_1 p_2 | \phi_A(x_A, p_A) \phi_B(x_B, p_B) \rangle_{\rm in}|^2 \\ &= \frac{4E_A E_B}{(2\pi)^{12}} G_1 G_2 \int d^3k_A d^3k_B d^3k'_A d^3k'_B \frac{\phi_A(\mathbf{k}_A - \mathbf{p}_A)\phi_B(\mathbf{k}_B - \mathbf{p}_B)\phi_A^*(\mathbf{k}'_A - \mathbf{p}_A)\phi_B^*(\mathbf{k}'_B - \mathbf{p}_B)}{\sqrt{16 E_{A,k} E_{B,k} E_{A,k'} E_{B,k'}}} \\ &\quad \times \exp(-i\mathbf{k}_A \cdot \mathbf{x}_A - i\mathbf{k}_B \cdot \mathbf{x}_B + i\mathbf{k}'_A \cdot \mathbf{x}_A + i\mathbf{k}'_B \cdot \mathbf{x}_B)(2\pi)^4 \delta^{(4)}(k'_A + k'_B - p_1 - p_2)(2\pi)^4 \delta^{(4)}(k_A + k_B - p_1 - p_2) \\ &\quad \times \mathcal{M}(\{k_A, k_B\} \to \{p_1, p_2\}) \mathcal{M}^*(\{k'_A, k'_B\} \to \{p_1, p_2\}), \end{aligned} \tag{11}$$

where $\phi_i(\mathbf{k}_i - \mathbf{p}_i)$ and $\phi_i(\mathbf{k}'_i - \mathbf{p}_i)$ for $i = A, B$ denote the incident wave packet amplitudes centered at $\mathbf{p}_i$, $E_{i,k} = \sqrt{|\mathbf{k}_i|^2 + m_i^2}$, $E_{i,k'} = \sqrt{|\mathbf{k}'_i|^2 + m_i^2}$ and $E_i = \sqrt{|\mathbf{p}_i|^2 + m_i^2}$ are energies for $i = A, B$. In Eq. (11) G_i $(i = 1, 2)$ denote distribution factors depending on particle types in the final state, we have $G_i = 1$ for the Boltzmann particles and $G_i = 1 \pm f_i(p_i)$ for bosons (upper sign) and fermions (lower sign). Note that

$f_i(p_i)$ can be in any other form in nonequilibrium cases. In (11) we have taken the following form for $|\phi_i(x_i, p_i)\rangle_{\text{in}}$ with $i = A, B$:

$$|\phi_i(x_i, p_i)\rangle_{\text{in}} = \int \frac{d^3k_i}{(2\pi)^3} \frac{1}{\sqrt{2E_{i,k}}} \phi_i(\mathbf{k}_i - \mathbf{p}_i) e^{-i\mathbf{k}_i\cdot\mathbf{x}_i} |\mathbf{k}_i\rangle_{\text{in}}. \tag{12}$$

Here we take the Gaussian form for the wave packet amplitude $\phi_i(\mathbf{k}_i - \mathbf{p}_i)$ as in (A10),

$$\phi_i(\mathbf{k}_i - \mathbf{p}_i) = \frac{(8\pi)^{3/4}}{\alpha_i^{3/2}} \exp\left[-\frac{(\mathbf{k}_i - \mathbf{p}_i)^2}{\alpha_i^2}\right], \tag{13}$$

where α_i denote the width parameters of the wave packet A or B. For simplicity we will set equal width for two incident particles (even for different species), $\alpha_A = \alpha_B = \alpha$.

We can also make the approximation of narrow wave packets, so we have $|\mathbf{k}_i| \approx |\mathbf{k}_i'| \approx |\mathbf{p}_i|$ for $i = A, B$ and then $\sqrt{E_{A,k}E'_{A,k}} \approx E_A$ and $\sqrt{E_{B,k}E'_{B,k}} \approx E_B$, and the energy factors in (11) drop out. By taking the integral over x_A and x_B and then the integral over on-shell momenta p_A, p_B, p_1, and p_2, we obtain the scattering or collision rate per unit volume,

$$\begin{aligned} R_{AB\to 12} = &\int \frac{d^3p_A}{(2\pi)^3 2E_A} \frac{d^3p_B}{(2\pi)^3 2E_B} \frac{d^3p_1}{(2\pi)^3 2E_1} \frac{d^3p_2}{(2\pi)^3 2E_2} \\ &\times \frac{1}{C_{AB}} \int d^4x_A d^4x_B \delta(\Delta t)\delta(\Delta x_L) \\ &\times f_A(x_A, p_A) f_B(x_B, p_B) G_1 G_2 |v_A - v_B| K. \end{aligned} \tag{14}$$

Now we use new variables to replace x_A and x_B,

$$\begin{aligned} X &= \tfrac{1}{2}(x_A + x_B), \\ y &= x_A - x_B. \end{aligned} \tag{15}$$

We can rewrite the integral over x_A and x_B in Eq. (14) as

$$\begin{aligned} I = &\int d^4x_A d^4x_B \delta(\Delta t)\delta(\Delta x_L) f_A(x_A, p_A) f_B(x_B, p_B) \\ &\times \exp(-i\mathbf{k}_A\cdot\mathbf{x}_A - i\mathbf{k}_B\cdot\mathbf{x}_B + i\mathbf{k}'_A\cdot\mathbf{x}_A + i\mathbf{k}'_B\cdot\mathbf{x}_B) \\ \approx &\int d^4X d^2\mathbf{b} f_A\left(X + \frac{y_T}{2}, p_A\right) f_B\left(X - \frac{y_T}{2}, p_B\right) \\ &\times \exp[i(\mathbf{k}'_A - \mathbf{k}_A)\cdot\mathbf{b}], \end{aligned} \tag{16}$$

where we have used $\mathbf{k}_A + \mathbf{k}_B - \mathbf{k}'_A - \mathbf{k}'_B = 0$ and $-\mathbf{k}_A + \mathbf{k}_B + \mathbf{k}'_A - \mathbf{k}'_B = 2(\mathbf{k}'_A - \mathbf{k}_A)$ implied by two delta functions in Eq. (11). In Eq. (16) we have integrated over $y^0 = \Delta t = t_A - t_B$ and $y_L = \Delta x_L = \hat{\mathbf{p}}_A\cdot(\mathbf{x}_A - \mathbf{x}_B)$ to remove two delta functions, then we are left with the integral over the transverse part $y_T^\mu = (0, \mathbf{b})$ with $\mathbf{b}$ being in the transverse direction. Because we work in the CMS in which all kinematic variables depend on the incident momenta in the laboratory frame, the impact parameter $\mathbf{b}$ in the CMS depends on (x_A, x_B) as well as $(\mathbf{p}_A, \mathbf{p}_B)$ in the laboratory frame through a boost velocity.

Now we define the constant C_{AB} in Eqs. (10) and (14) as $C_{AB} \equiv \int d^4X = t_X \Omega_{\text{int}}$ so that the final results have the right dimension. Here t_X and Ω_{int} are the local time and space volume for the interaction respectively. Note that $C_{AB}^{-1}\int d^4X(\dots)$ plays the role of the average over X or $\langle(\dots)\rangle_X$. If we take the limit $t_X\Omega_{\text{int}} \to 0$, we obtain the local rate per unit volume from Eq. (14),

$$\begin{aligned} \frac{d^4N_{AB\to 12}}{dX^4} = &\frac{1}{(2\pi)^4} \int \frac{d^3p_A}{(2\pi)^3 2E_A} \frac{d^3p_B}{(2\pi)^3 2E_B} \frac{d^3p_1}{(2\pi)^3 2E_1} \frac{d^3p_2}{(2\pi)^3 2E_2} |v_A - v_B| G_1 G_2 \int d^3k_A d^3k_B d^3k'_A d^3k'_B \\ &\times \phi_A(\mathbf{k}_A - \mathbf{p}_A)\phi_B(\mathbf{k}_B - \mathbf{p}_B)\phi_A^*(\mathbf{k}'_A - \mathbf{p}_A)\phi_B^*(\mathbf{k}'_B - \mathbf{p}_B)\delta^{(4)}(k'_A + k'_B - p_1 - p_2)\delta^{(4)}(k_A + k_B - p_1 - p_2) \\ &\times \mathcal{M}(\{k_A, k_B\} \to \{p_1, p_2\})\mathcal{M}^*(\{k'_A, k'_B\} \to \{p_1, p_2\}) \int d^2\mathbf{b} f_A\left(X + \frac{y_T}{2}, p_A\right) f_B\left(X - \frac{y_T}{2}, p_B\right) \exp[i(\mathbf{k}'_A - \mathbf{k}_A)\cdot\mathbf{b}], \end{aligned} \tag{17}$$

where $N_{AB\to 12}$ is the number of scatterings. We emphasize again that all quantities in Eq. (17) are defined in the CMS of two incident particles (we have suppressed the index c).

IV. POLARIZATION RATE FOR SPIN-1/2 PARTICLES FROM COLLISIONS

In this section we will generalize the previous section for spin-0 particles to spin-1/2 ones. Our purpose is to derive the polarization rate from collisions in a system of particles of multispecies. We assume that particle distributions in phase space are independent of spin states, so the spin dependence comes only from scatterings of particles carrying the spin degree of freedom.

As a simple example to illustrate the idea of the polarization arising from collisions, we consider a fluid with the three-vector fluid velocity in the z direction v_z that depends on x, which we denote as $v_z(x)$. We assume $dv_z(x)/dx > 0$. In the comoving frame of any fluid cell in the range $[x - \Delta x/2, x + \Delta x/2]$ where Δx is a small distance, the fluid velocity at $x \pm \Delta x/2$ is $\pm(dv_z(x)/dx)\Delta x$, forming a rotation or local orbital angular momentum (OAM) pointing to the $-y$ direction. Due to the spin-orbit coupling, the scattering of two unpolarized particles with velocity $\pm(dv_z(x)/dx)\Delta x$ and impact parameter Δx will polarize the particles in the final state along the direction of the local OAM. It has been proved that the polarization cross section is proportional to $\mathbf{s}\cdot\mathbf{n}_c$, where $\mathbf{s}$ is the spin quantization (polarization) direction and $\mathbf{n}_c = \hat{\mathbf{b}}_c \times \hat{\mathbf{p}}_c$ is the direction of the reaction plane (the local OAM) in the CMS of the scattering, where $\hat{\mathbf{b}}_c$ and $\hat{\mathbf{p}}_c$ are the direction of the impact parameter and the incident momentum respectively. This is what happens in one scattering. In a thermal system with collective motion, there are many scatterings whose reaction planes point to almost random directions, but on average the direction of the reaction plane points to that of the local rotation or vorticity. To calculate the polarization in a thermal system with collective motion, we have to take a convolution of distribution functions and polarized scattering amplitudes similar to (17).

In this section we will distinguish quantities in the CMS and laboratory frame, i.e., we will resume the subscript c for all CMS quantities, while quantities in the laboratory frame do not have the subscript c.

Now we consider a scattering process $A+B\rightarrow 1+2$ where the incident and outgoing particles are in the spin state labeled by s_A, s_B, s_1, and s_2 ($s_i=\pm 1/2$, $i=A,B,1,2$) respectively. The quantization direction of the spin state is chosen to be along the direction of the reaction plane in the CMS of the scattering. The polarization rate per unit volume for particle 2 in the final state is given by

$$\begin{aligned}\frac{d^4\mathbf{P}_{AB\rightarrow 12}(X)}{dX^4} &= \frac{1}{(2\pi)^4}\int\frac{d^3p_{c,A}}{(2\pi)^3 2E_{c,A}}\frac{d^3p_{c,B}}{(2\pi)^3 2E_{c,B}}\frac{d^3p_{c,1}}{(2\pi)^3 2E_{c,1}}\frac{d^3p_{c,2}}{(2\pi)^3 2E_{c,2}}|v_{c,A}-v_{c,B}|G_1G_2\int d^3k_{c,A}d^3k_{c,B}d^3k'_{c,A}d^3k'_{c,B}\\ &\quad\times\phi_A(\mathbf{k}_{c,A}-\mathbf{p}_{c,A})\phi_B(\mathbf{k}_{c,B}-\mathbf{p}_{c,B})\phi_A^*(\mathbf{k}'_{c,A}-\mathbf{p}_{c,A})\phi_B^*(\mathbf{k}'_{c,B}-\mathbf{p}_{c,B})\\ &\quad\times\delta^{(4)}(k'_{c,A}+k'_{c,B}-p_{c,1}-p_{c,2})\delta^{(4)}(k_{c,A}+k_{c,B}-p_{c,1}-p_{c,2})\\ &\quad\times\int d^2\mathbf{b}_c f_A\left(X_c+\frac{y_{c,T}}{2},p_{c,A}\right)f_B\left(X_c-\frac{y_{c,T}}{2},p_{c,B}\right)\exp[i(\mathbf{k}'_{c,A}-\mathbf{k}_{c,A})\cdot\mathbf{b}_c]\\ &\quad\times\sum_{s_A,s_B,s_1,s_2}2s_2\mathbf{n}_c\mathcal{M}(\{s_A,k_{c,A};s_B,k_{c,B}\}\rightarrow\{s_1,p_{c,1};s_2,p_{c,2}\})\mathcal{M}^*(\{s_A,k'_{c,A};s_B,k'_{c,B}\}\rightarrow\{s_1,p_{c,1};s_2,p_{c,2}\}),\end{aligned}\tag{18}$$

where $\mathbf{P}_{AB\rightarrow 12}$ denotes the polarization vector and $\mathbf{n}_c=\hat{\mathbf{b}}_c\times\hat{\mathbf{p}}_{c,A}$ is the direction of the reaction plane in the CMS of the scattering which is also the quantization direction of the spin. In the second to the last line of Eq. (18), the summation of $2s_2\mathcal{M}(\ldots,s_2)\mathcal{M}^*(\ldots,s_2)$ over $s_2=\pm 1/2$ gives the polarized amplitude squared for particle 2 in the final state, and the factor 2 arises from the normalization convention for the polarization that makes it in the range $[-1,1]$ instead of $[-1/2,1/2]$. Equation (18) is one of our main results.

V. QUARK/ANTIQUARK POLARIZATION RATE IN A QUARK-GLUON PLASMA OF LOCAL EQUILIBRIUM IN MOMENTUM

In this section we will calculate the quark/antiquark polarization rate from all 2-to-2 parton (quark or gluon) collisions in a quark-gluon plasma (QGP) of local equilibrium in momentum but not in spin. We assume that the QGP is a multicomponent fluid with the same fluid velocity $u(x)$ as a function of space-time for all partons. The partons in a fluid cell follow a thermal distribution in momentum in its comoving frame with the local temperature $T(x)$. We assume that the phase space distribution $f(x,p)$ depends on $x^\mu=(t,\mathbf{x})$ through the fluid velocity $u^\mu(x)$ in the form $f(x,p)=f[\beta(x)p\cdot u(x)]$ where $p^\mu=(E_p,\mathbf{p})$ is an on-shell four-momentum of the parton and $\beta(x)\equiv 1/T(x)$.

We consider the scattering, $A+B\rightarrow 1+2$, where A and B denote two incident partons in the wave packet form localized at x_A and x_B respectively, and "1" and "2" denote two outgoing partons in momentum states. In order to calculate the polarization rate from the collision of two wave packets displaced by an impact parameter by Eq. (18), we must work in the CMS of the incident partons for each collision. Note that many collisions take place in the system at different space-time; the CMS of each collision depends on the momenta of incident partons which vary from collision to collision. In one collision, the phase space distributions for incident partons (denoted as $i=A,B$) can be written in the form

$$\begin{aligned}f_i(x_c,p_c) &= f_i[\beta(x_c)p_c\cdot u_c(x_c)]\\ &= f_i[\beta(x)p\cdot u(x)]\\ &= f_i(x,p),\end{aligned}\tag{19}$$

where x, p are the space-time and momentum in the laboratory frame respectively, while x_c, p_c are their corresponding values in the CMS of A and B in this collision which depend on p_A and p_B in the heat bath (laboratory frame) through the boost velocity, and $u_c^\mu(x_c)$ denotes the fluid velocity in the CMS as a function of the space-time in the CMS.

A. Polarization rate

We now apply Eq. (18) to 2-to-2 parton scatterings. For simplicity we assume that the phase space distributions of incident partons follow the Boltzmann distribution, i.e., $f(x,p)=\exp[-\beta(x)p\cdot u(x)]$, so we have $G_1G_2=1$ in (18). Also we assume that $y_{c,T}$ is small compared with X_c so that we can make an expansion in $y_{c,T}$ for the distributions, the details are given in Appendix B. The relevant contribution in the linear or first order in $y_{c,T}$ involves the term

$y^{\mu}_{c,T}[\partial(\beta u_{c,\rho})/\partial X^{\mu}_c]p^{\rho}_{c,A}$ which can be rewritten as

$$y^{\mu}_{c,T}p^{\rho}_{c,A}\frac{\partial(\beta u_{\rho})}{\partial X^{\mu}_c} = -\frac{1}{2}L^{\mu\rho}_{(c)}\omega^{(c)}_{\mu\rho} + \frac{1}{4}y^{\{\mu}_{c,T}p^{\rho\}}_{c,A}\left[\frac{\partial(\beta u_{c,\rho})}{\partial X^{\mu}_c} + \frac{\partial(\beta u_{c,\mu})}{\partial X^{\rho}_c}\right], \quad (20)$$

where $L^{\mu\rho}_{(c)} \equiv y^{[\mu}_{c,T}p^{\rho]}_{c,A}$ is the OAM tensor, $\omega^{(c)}_{\mu\rho} \equiv -(1/2)[\partial^{X_c}_{\mu}(\beta u_{c,\rho}) - \partial^{X_c}_{\rho}(\beta u_{c,\mu})]$ is the thermal vorticity tensor, and $y^{\{\mu}_{c,T}p^{\rho\}}_{c,A} \equiv y^{\mu}_{c,T}p^{\rho}_{c,A} + y^{\rho}_{c,T}p^{\mu}_{c,A}$, all in the CMS. The derivation of Eq. (20) is given in Eq. (B2). Note that the OAM-vorticity coupling $L^{\mu\rho}_{(c)}\omega^{(c)}_{\mu\rho}$ shows up in the $y_{c,T}$ expansion, which can be converted to the spin-vorticity coupling through polarized parton scattering amplitudes encoding the spin-orbit coupling effect, as we will show shortly. The second term in Eq. (20) involves the symmetric part of the thermal velocity derivatives in space-time, which is assumed to vanish in thermal equilibrium for the spin, known as the Killing condition [12–14,17]. In this paper, however, we do not assume the thermal equilibrium for the spin degree of freedom, so we keep this symmetric term in the calculation.

Keeping the first order term in the $y_{c,T}$ expansion and neglecting the zeroth order term, which is irrelevant, Eq. (18) can be simplified as

$$\frac{d^4\mathbf{P}_{AB\to 12}(X)}{dX^4} = -\frac{1}{(2\pi)^4}\int\frac{d^3p_A}{(2\pi)^3 2E_A}\frac{d^3p_B}{(2\pi)^3 2E_B}\frac{d^3p_{c,1}}{(2\pi)^3 2E_{c,1}}\frac{d^3p_{c,2}}{(2\pi)^3 2E_{c,2}}|v_{c,A}-v_{c,B}|\int d^3k_{c,A}d^3k_{c,B}d^3k'_{c,A}d^3k'_{c,B}$$
$$\times\phi_A(\mathbf{k}_{c,A}-\mathbf{p}_{c,A})\phi_B(\mathbf{k}_{c,B}-\mathbf{p}_{c,B})\phi^*_A(\mathbf{k}'_{c,A}-\mathbf{p}_{c,A})\phi^*_B(\mathbf{k}'_{c,B}-\mathbf{p}_{c,B})$$
$$\times\delta^{(4)}(k'_{c,A}+k'_{c,B}-p_{c,1}-p_{c,2})\delta^{(4)}(k_{c,A}+k_{c,B}-p_{c,1}-p_{c,2})$$
$$\times\frac{1}{2}\int d^2\mathbf{b}_c\exp[i(\mathbf{k}'_{c,A}-\mathbf{k}_{c,A})\cdot\mathbf{b}_c]\mathbf{b}_{c,j}[\Lambda^{-1}]^{\nu}_{\ j}\frac{\partial(\beta u_{\rho})}{\partial X^{\nu}}\left(p^{\rho}_A-p^{\rho}_B\right)f_A(X,p_A)f_B(X,p_B)\Delta I^{AB\to 12}_M\mathbf{n}_c, \quad (21)$$

where we have used $d^3p_{c,i}/E_{c,i} = d^3p_i/E_i$ for $i = A, B$, the Lorentz transformation matrix is defined by $\partial X^{\nu}/\partial X^{\mu}_c = [\Lambda^{-1}]^{\nu}_{\ \mu} = \Lambda_{\mu}^{\ \nu}$, the minus sign in the right-hand side comes from $df_i(X,p_i)/d(\beta u\cdot p_i)$ for $i = A, B$, and $\Delta I^{AB\to 12}_M$ is defined by

$$\Delta I^{AB\to 12}_M = \sum_{s_A,s_B,s_1,s_2}\sum_{\text{color}}2s_2\mathcal{M}(\{s_A,k_{c,A};s_B,k_{c,B}\}\to\{s_1,p_{c,1};s_2,p_{c,2}\})$$
$$\times\mathcal{M}^*(\{s_A,k'_{c,A};s_B,k'_{c,B}\}\to\{s_1,p_{c,1};s_2,p_{c,2}\}), \quad (22)$$

where the factor 2 arises from the normalization convention for the polarization. Note that in the above formula there is a sum over color degrees of freedom of all incident and outgoing partons. We may write $\Delta I^{AB\to 12}_M\mathbf{n}_c$ as

$$\Delta I^{AB\to 12}_M\mathbf{n}_c = \Delta I^{AB\to 12}_M(\hat{\mathbf{b}}_c\times\hat{\mathbf{p}}_{c,A}) = i(\hat{\mathbf{b}}_c\cdot\mathbf{I}_c)\mathbf{e}_{c,i}\epsilon_{ikh}\hat{\mathbf{b}}_{c,k}\hat{\mathbf{p}}^h_{c,A} = i\mathbf{e}_{c,i}\epsilon_{ikh}\hat{\mathbf{p}}^h_{c,A}\mathbf{I}_{c,l}\hat{\mathbf{b}}_{c,l}\hat{\mathbf{b}}_{c,k}, \quad (23)$$

where $\mathbf{e}_{c,i}$ ($i = x, y, z$) are the basis vectors in the CMS, and $\Delta I^{AB\to 12}_M$ can be put into the form $i\hat{\mathbf{b}}_c\cdot\mathbf{I}_c$; in this way we can single out the direction $\hat{\mathbf{b}}_c$ out of $\Delta I^{AB\to 12}_M$ [see Eq. (40) for an example of what $\mathbf{I}_c$ looks like].

Substituting Eq. (23) into Eq. (21), completing the integration over $\mathbf{b}_c$, and removing delta functions by integration, we obtain

$$\frac{d^4\mathbf{P}_{AB\to 12}(X)}{dX^4} = \frac{\pi}{(2\pi)^4}\frac{\partial(\beta u_{\rho})}{\partial X^{\nu}}\int\frac{d^3p_A}{(2\pi)^3 2E_A}\frac{d^3p_B}{(2\pi)^3 2E_B}|v_{c,A}-v_{c,B}|[\Lambda^{-1}]^{\nu}_{\ j}\mathbf{e}_{c,i}\epsilon_{ikh}\hat{\mathbf{p}}^h_{c,A}f_A(X,p_A)f_B(X,p_B)\left(p^{\rho}_A-p^{\rho}_B\right)$$
$$\times\int\frac{d^3p_{c,1}}{(2\pi)^3 2E_{c,1}}\frac{d^3p_{c,2}}{(2\pi)^3 2E_{c,2}}d^2\mathbf{k}^T_{c,A}d^2\mathbf{k}'^T_{c,A}\sum_{j_1,j_2=1,2}\frac{1}{\left|\mathrm{Ja}\left[k^L_{c,A}(j_1)\right]\right|}\cdot\frac{1}{\left|\mathrm{Ja}\left[k'^L_{c,A}(j_2)\right]\right|}$$
$$\times\phi_A(\mathbf{k}_{c,A}-\mathbf{p}_{c,A})\phi_B(\mathbf{k}_{c,B}-\mathbf{p}_{c,B})\phi^*_A(\mathbf{k}'_{c,A}-\mathbf{p}_{c,A})\phi^*_B(\mathbf{k}'_{c,B}-\mathbf{p}_{c,B})$$
$$\times\mathbf{I}_{c,l}\frac{1}{a^3}\left\{Q^L_{jkl}\left[-2+2J_0(w_0)+w_0J_1(w_0)+w_0^2J_2(w_0)\right]+Q^T_{jkl}[2-2J_0(w_0)-w_0J_1(w_0)]\right\}. \quad (24)$$

Here we have used

$$Q^L_{jkl} = \frac{\mathbf{a}_l\mathbf{a}_j\mathbf{a}_k}{a^3},$$
$$Q^T_{jkl} = \frac{1}{a^3}(a^2\mathbf{a}_k\delta_{lj}+a^2\mathbf{a}_l\delta_{jk}+a^2\mathbf{a}_j\delta_{lk}-3\mathbf{a}_l\mathbf{a}_j\mathbf{a}_k), \quad (25)$$

with $\mathbf{a}\equiv\mathbf{k}'_{c,A}-\mathbf{k}_{c,A}$ and $a = |\mathbf{a}|$, $w_0 = ab_0$ with b_0 being the upper limit or cutoff of b_c, J_i for $i = 0, 1, 2$ are Bessel functions, $\mathbf{k}_{c,B} = \mathbf{p}_{c,1}+\mathbf{p}_{c,2}-\mathbf{k}_{c,A}$, $\mathbf{k}'_{c,B} = \mathbf{p}_{c,1}+\mathbf{p}_{c,2}-\mathbf{k}'_{c,A}$, $\mathrm{Ja}(k^L_{c,A})$ and $\mathrm{Ja}(k'^L_{c,A})$ are Jacobians for the longitudinal momenta $k^L_{c,A}$ and $k'^L_{c,A}$ and are given by

$$\mathrm{Ja}\left(k^L_{c,A}\right) = k^L_{c,A}\left(\frac{1}{E_{c,A}}+\frac{1}{E_{c,B}}\right)-\frac{1}{E_{c,B}}\left(p^L_{c,1}+p^L_{c,2}\right),$$
$$\mathrm{Ja}\left(k'^L_{c,A}\right) = k'^L_{c,A}\left(\frac{1}{E'_{c,A}}+\frac{1}{E'_{c,B}}\right)-\frac{1}{E'_{c,B}}\left(p^L_{c,1}+p^L_{c,2}\right), \quad (26)$$

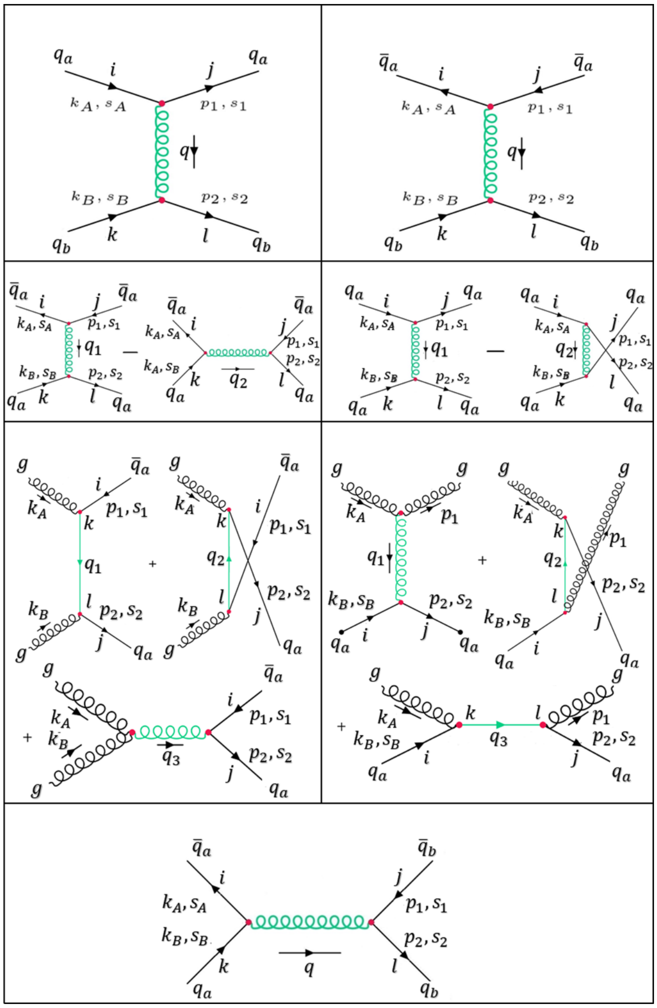

FIG. 2. The Feynman diagrams of all 2-to-2 parton scatterings at the tree level with at least one quark in the final state. We calculate the polarization of the quark (the second parton) in the final state. Here a and b denote the quark flavor, $s_i = \pm 1/2$ $(i = A, B, 1, 2)$ denote the spin states, k_i $(i = A, B, 1, 2)$ denote the momenta, q, q_1, q_2, q_3 denote the momenta in propagators. The processes for antiquark polarization can be obtained by making a particle-antiparticle transformation.

and $k^L_{c,A}(j_1)$ and $k'^L_{c,A}(j_2)$ with $j_1, j_2 = 1, 2$ are two roots of the energy conservation equation $E_{c,A} + E_{c,B} - E_{c,1} - E_{c,2} = 0$ and $E'_{c,A} + E'_{c,B} - E_{c,1} - E_{c,2} = 0$ respectively. In (24) and (25) latin indices label spatial components in the CMS. The derivation of (24) is given in Appendix D.

In a system of gluons and quarks with multiflavors, there are many 2-to-2 parton scatterings with at least one quark in the final state. The quark polarization rate for a specific flavor reads

$$\frac{d^4\mathbf{P}_q(X)}{dX^4} = \sum_{A,B,1=\{q_a,\bar{q}_a,g\}} \frac{d^4\mathbf{P}_{AB\to 1q}(X)}{dX^4}, \tag{27}$$

where $d^4\mathbf{P}_{AB\to 1q}(X)/dX^4$ is given by Eq. (24), and 2-to-2 parton scatterings are listed in Fig. 2. The antiquark polarization rate can be similarly obtained.

B. Polarized amplitudes for quarks/antiquarks in 2-to-2 parton scatterings

In this subsection we will derive the polarized amplitudes for quarks in 2-to-2 parton scatterings. The Feynman diagrams of all 2-to-2 parton scatterings at the tree level with at least one quark in the final state are shown in Fig. 2. For antiquark polarization, we can make particle-antiparticle transformation in all processes listed in Fig. 2, for example, $q_a q_b \to q_a q_b$ becomes $\bar{q}_a\bar{q}_b \to \bar{q}_a\bar{q}_b$, $\bar{q}_a q_b \to \bar{q}_a q_b$ becomes $q_a\bar{q}_b \to q_a\bar{q}_b$, $gg \to \bar{q}_a q_a$ becomes $gg \to q_a\bar{q}_a$, etc. In this subsection, we discuss polarized amplitudes for quarks; those for antiquarks can be easily obtained.

In order to obtain the quark polarization, we sum over the spin states of all partons in the scattering except one quark in the final state. For simplicity of the calculation, we assume that the quark masses are equal for all flavors and the external gluon is massless. We introduce a small mass in the gluon propagator in the t channel to regulate the possible divergence.

In this subsection, all variables are defined in the CMS. For notational simplicity we will suppress the subscript c; for example, p_A actually means p_{cA}.

We take the quark-quark scattering $q_a q_b \to q_a q_b$ with $a \neq b$ (different flavor) as an example to demonstrate how to derive the polarized scattering amplitude which depends on the spin state of the quark in the final state. The Feynman diagram of this process is shown in Fig. 2. The spin-momentum configurations are shown in the diagram. We can then write down the corresponding amplitudes following the Feynman rule,

$$\begin{aligned} I_1 &= -i\mathcal{M}(\{s_A, k_A; s_B, k_B\} \to \{s_1, p_1; s_2, p_2\}) \\ &= ig_s^2 t^c_{ji} t^c_{lk} \frac{1}{q^2}[\bar{u}(s_1, p_1)\gamma^\mu u(s_A, k_A)][\bar{u}(s_2, p_2)\gamma_\mu u(s_B, k_B)], \\ I_2 &= -i\mathcal{M}(\{s_A, k'_A; s_B, k'_B\} \to \{s_1, p_1; s_2, p_2\}) \\ &= ig_s^2 t^d_{ji} t^d_{lk} \frac{1}{q'^2}[\bar{u}(s_1, p_1)\gamma^\nu u(s_A, k'_A)][\bar{u}(s_2, p_2)\gamma_\nu u(s_B, k'_B)], \end{aligned} \tag{28}$$

where g_s is the strong coupling constant, $i, j, k, l = 1, 2, 3$ denote the fundamental colors of quarks, $c, d = 1, \dots, 8$ denote the adjoint colors of gluons, t^c and t^d are generators of SU(N_c) in fundamental representation satisfying $[t^a, t^b] = if^{abc}t^c$, $q = k_A - p_1$, and $q' = k'_A - p_1$. We obtain the product $I_1 I_2^*$ as

$$\begin{aligned} &I_M^{q_a q_b \to q_a q_b}(s_2) \\ &= \sum_{s_A, s_B, s_1} \sum_{i,j,k,l} \mathcal{M}(\{s_A, k_A; s_B, k_B\} \to \{s_1, p_1; s_2, p_2\}) \\ &\quad \times \mathcal{M}^*(\{s_A, k'_A; s_B, k'_B\} \to \{s_1, p_1; s_2, p_2\}) \\ &= C_{q_a q_b \to q_a q_b} g_s^4 m^2 \frac{1}{q^2 q'^2} \\ &\quad \times \mathrm{Tr}\big[(p_1 \cdot \gamma + m)\gamma^\mu \Lambda_{1/2}(-\mathbf{k}_A)(\gamma_0 + 1)\Lambda^{-1}_{1/2}(-\mathbf{k}'_A)\gamma^\nu\big] \\ &\quad \times \mathrm{Tr}\big[\Pi(s_2, n)(p_2 \cdot \gamma + m)\gamma_\mu \Lambda_{1/2}(-\mathbf{k}_B)(\gamma_0 + 1) \\ &\quad \times \Lambda^{-1}_{1/2}(-\mathbf{k}'_B)\gamma_\nu\big]. \end{aligned} \tag{29}$$

TABLE I. Color factors for all 2-to-2 processes with at least one final quark. The constants which appear in color factors are $d_F = N_c$, $d_A = N_c^2 - 1$, $C_F = (N_c^2 - 1)/(2N_c)$, and $C_A = 3$ with $N_c = 3$.

Color factors	Color factors in scattering processes
$d_F^2 C_F^2 / d_A$	$C_{q_a q_b \to q_a q_b}$, $C_{\bar{q}_a q_b \to \bar{q}_a q_b}$, $C^{(1)}_{\bar{q}_a q_a \to \bar{q}_a q_a}$, $C^{(1)}_{q_a q_a \to q_a q_a}$, $C_{\bar{q}_a q_a \to \bar{q}_b q_b}$
$d_F C_F^2$	$C^{(1)}_{gg \to \bar{q}_a q_a}$, $C^{(3)}_{g q_a \to g q_a}$
$(C_F - C_A/2) d_F C_F$	$C^{(2)}_{\bar{q}_a q_a \to \bar{q}_a q_a}$, $C^{(2)}_{q_a q_a \to q_a q_a}$, $C^{(2)}_{gg \to \bar{q}_a q_a}$, $C^{(4)}_{g q_a \to g q_a}$
$\frac{1}{4} d_A C_A$	$C^{(2)}_{g q_a \to g q_a}$, $C^{(3)}_{gg \to \bar{q}_a q_a}$
$d_F C_F C_A$	$C^{(1)}_{g q_a \to g q_a}$, $C^{(4)}_{gg \to \bar{q}_a q_a}$

In Eq. (29) we have used the notation $p \cdot \gamma \equiv p_\rho \gamma^\rho$, a sum over all spins except s_2 and over all colors of quarks and gluons have been taken, and $C_{q_a q_b \to q_a q_b}$ is the color factor for this process given in Table I. In the last two lines of Eq. (29), $\Lambda_{1/2}$ and $\Lambda_{1/2}^{-1}$ are the Lorentz transformation matrices for spinors defined in Eq. (E10), $\Pi(s_2, n) = (1 + s_2 \gamma_5 n^\sigma \gamma_\sigma)/2$ is the spin projector where $n^\sigma = (0, \mathbf{n})$ is the spin quantization four-vector in the CMS with $\mathbf{n} = \hat{\mathbf{b}} \times \hat{\mathbf{p}}_A$, and we have applied Eqs. (E13) and (E18). From Eq. (29), we obtain the difference of $I_M^{q_a q_b \to q_a q_b}$ between the spin state $s_2 = 1/2$ and $s_2 = -1/2$ for q_b,

$$
\begin{aligned}
\Delta I_M^{q_a q_b \to q_a q_b} &= I_M^{q_a q_b \to q_a q_b}(s_2 = 1/2) - I_M^{q_a q_b \to q_a q_b}(s_2 = -1/2) \\
&= C_{q_a q_b \to q_a q_b} g_s^4 m^2 \frac{1}{q^2 q'^2} \\
&\quad \times \mathrm{Tr}\big[(p_1 \cdot \gamma + m)\gamma^\mu \Lambda_{1/2}(-\mathbf{k}_A)(\gamma_0 + 1)\Lambda_{1/2}^{-1}(-\mathbf{k}'_A)\gamma^\nu\big] \\
&\quad \times \mathrm{Tr}\big[\gamma_5 (n \cdot \gamma)(p_2 \cdot \gamma + m)\gamma_\mu \Lambda_{1/2}(-\mathbf{k}_B)(\gamma_0 + 1) \\
&\quad \times \Lambda_{1/2}^{-1}(-\mathbf{k}'_B)\gamma_\nu\big]. \qquad (30)
\end{aligned}
$$

The expansion of $\Delta I_M^{q_a q_b \to q_a q_b}$ gives about 200 terms. In accordance with Eq. (E10), $\Lambda_{1/2}(\mathbf{p})$ depends on the rapidity η_p and the momentum direction $\hat{\mathbf{p}}$, where η_p is related to the energy momentum by $E_p = m \cosh(\eta_p)$ and $|\mathbf{p}| = m \sinh(\eta_p)$. So the contracted trace part of $\Delta I_M^{q_a q_b \to q_a q_b}$ can be expressed as a function of $(\hat{\mathbf{k}}_A, \hat{\mathbf{k}}'_A, \hat{\mathbf{k}}_B, \hat{\mathbf{k}}'_B)$ and $(\eta_{kA}, \eta'_{kA}, \eta_{kB}, \eta'_{kB})$.

The polarized amplitudes for quarks in all 2-to-2 parton scatterings listed in Fig. 2 are given in Appendix F, which results in more than 5000 terms. Here we give an estimate of how many terms there are in each process: $\Delta I_M^{gg \to \bar{q}_a q_a}$ gives 136 terms, $\Delta I_M^{g q_a \to g q_a}$ gives 2442 terms, $\Delta I_M^{\bar{q}_a q_a \to \bar{q}_a q_a}$ gives 874 terms, $\Delta I_M^{\bar{q}_a q_a \to \bar{q}_b q_b}$ gives 40 terms, $\Delta I_M^{\bar{q}_a q_b \to \bar{q}_a q_b}$ gives 210 terms, $\Delta I_M^{q_a q_b \to q_a q_b}$ gives 210 terms, $\Delta I_M^{q_a q_a \to q_a q_a}$ gives 1156 terms. It is hard to see the physics behind such huge number of terms unless we make an appropriate approximation.

C. Evaluation of polarized amplitudes for quarks/antiquarks

The evaluation of contracted traces of quark polarized amplitudes are very complicated. This has been done with the help of FeynCalc [67,68]. There are about 10^4 terms in the expansion of contracted traces for 2-to-2 parton scatterings.

In this subsection, all variables are defined in the CMS; for notational simplicity we will suppress the subscript c if not explicitly specified—for example, p_A actually means p_{cA}.

In order to show the physics in the midst of the huge number of terms, we have to make an appropriate approximation. As we know that the incident particles are treated as wave packets in order to describe scatterings displaced by impact parameters, a realistic approximation is that the wave packets are assumed to be narrow, i.e., the width is much smaller than the center momenta of the wave packet in Eq. (13). In the extreme case that the width of the wave packet is zero, we recover the normal scattering of plane waves. Since the positions of incident particles can be anywhere in plane waves, on average the relative OAM of two incident particles is zero, leading to the vanishing polarization of final state particles. This fact can be verified by setting

$$
\begin{aligned}
&\hat{\mathbf{k}}_A = \hat{\mathbf{k}}'_A = \hat{\mathbf{p}}_A, \quad \hat{\mathbf{k}}_B = \hat{\mathbf{k}}'_B = -\hat{\mathbf{p}}_A, \\
&\mathbf{p}_1 = -\mathbf{p}_2, \quad \eta_A = \eta_B = \eta'_A = \eta'_B
\end{aligned} \qquad (31)
$$

in the trace part in Eq. (30); then we have $\Delta I_M^{q_a q_b \to q_a q_b} = 0$.

The above result is of the zeroth order; now we turn to the first order in the deviation from momenta in (31). We expand $(\hat{\mathbf{k}}_A, \hat{\mathbf{k}}'_A, \hat{\mathbf{k}}_B, \hat{\mathbf{k}}'_B)$ about their central values $(\hat{\mathbf{p}}_A, \hat{\mathbf{p}}_A, -\hat{\mathbf{p}}_A, -\hat{\mathbf{p}}_A)$ and $(\eta_{kA}, \eta'_{kA}, \eta_{kB}, \eta'_{kB})$ about their central values $(\eta_{pA}, \eta_{pA}, \eta_{pA}, \eta_{pA})$ to the first order in the differences,

$$
\begin{aligned}
&\hat{\mathbf{k}}_A \to \hat{\mathbf{p}}_A + \boldsymbol{\Delta}_A, \quad \hat{\mathbf{k}}_B \to -\hat{\mathbf{p}}_A + \boldsymbol{\Delta}_B, \\
&\hat{\mathbf{k}}'_A \to \hat{\mathbf{p}}_A + \boldsymbol{\Delta}'_A, \quad \hat{\mathbf{k}}'_B \to -\hat{\mathbf{p}}_A + \boldsymbol{\Delta}'_B, \\
&\eta_{kA} = \eta_{pA} + \Delta\eta_{kA}, \\
&\eta'_{kA} = \eta_{pA} + \Delta\eta'_{kA}, \\
&\eta_{kB} = \eta_{pA} + \Delta\eta_{kB}, \\
&\eta'_{kB} = \eta_{pA} + \Delta\eta'_{kB},
\end{aligned} \qquad (32)
$$

where the first order quantities are denoted with Δ (for example, $\boldsymbol{\Delta}_A$, $\Delta\eta_{kA}$). We also expand $(E_1, \mathbf{p}_1, E_2, \mathbf{p}_2)$ at $(E_0, \mathbf{p}_0, E_0, -\mathbf{p}_0)$,

$$
\begin{aligned}
&E_1 \to E_0 + \Delta_1, \quad E_2 \to E_0 + \Delta_2, \\
&\mathbf{p}_1 \to \mathbf{p}_0 + \boldsymbol{\Delta}_1, \quad \mathbf{p}_2 \to -\mathbf{p}_0 + \boldsymbol{\Delta}_1.
\end{aligned} \qquad (33)
$$

The delta functions in Eq. (21) lead to

$$
\mathbf{k}_A + \mathbf{k}_B = \mathbf{k}'_A + \mathbf{k}'_B = \mathbf{p}_1 + \mathbf{p}_2. \qquad (34)
$$

So $\boldsymbol{\Delta}_1$ in (33) can be determined by

$$
\boldsymbol{\Delta}_1 = \tfrac{1}{2}(\mathbf{k}_A + \mathbf{k}_B), \qquad (35)
$$

and $\mathbf{p}_0$ determined by

$$
\mathbf{p}_0 = \tfrac{1}{2}(\mathbf{p}_1 - \mathbf{p}_2). \qquad (36)
$$

Note that once $\mathbf{p}_0$ and $\boldsymbol{\Delta}_1$ are given, E_0, Δ_1, Δ_2 satisfy

$$
\begin{aligned}
&(E_0 + \Delta_1)^2 = (\mathbf{p}_0 + \boldsymbol{\Delta}_1)^2 + m_1^2, \\
&(E_0 + \Delta_2)^2 = (-\mathbf{p}_0 + \boldsymbol{\Delta}_1)^2 + m_2^2.
\end{aligned} \qquad (37)
$$

So we have a freedom to choose the value of E_0. Then we use (32) and (33) in the contracted trace part in Eq. (30) and expand it to the first order in Δ quantities. Still, the final result has many terms but all terms of $\Delta_1,\ \Delta_2$, and $\boldsymbol{\Delta}_1$ cancel out.

In order to further simplify the contracted trace part in Eq. (30), we use the property that the first order contributions do not have terms of Δ_1, Δ_2, $\boldsymbol{\Delta}_1$ by setting

$$\begin{aligned}\mathbf{p}_1 &= \mathbf{p}_0,\\ \mathbf{p}_2 &= -\mathbf{p}_0,\end{aligned} \tag{38}$$

which leads to $\mathbf{k}_A+\mathbf{k}_B=\mathbf{k}'_A+\mathbf{k}'_B=0$ and then

$$\begin{aligned}\hat{\mathbf{k}}_A &= -\hat{\mathbf{k}}_B, \quad \hat{\mathbf{k}}'_A = -\hat{\mathbf{k}}'_B,\\ \eta_{kA} &= \eta_{kB}, \quad \eta'_{kA} = \eta'_{kB}.\end{aligned} \tag{39}$$

Using (38) and (39) in the contracted trace part in Eq. (30) for $q_a q_b \to q_a q_b$, we obtain a shorter series of 31 terms,

$$\begin{aligned}\mathrm{Tr}^2_{\mathrm{q_a q_b \to q_a q_b}} =\ & 16i(\mathbf{n}\times\mathbf{p}_1)\cdot\hat{\mathbf{k}}_A\big[5c_A s_A c'_A s'_A \mathbf{p}_1\cdot\hat{\mathbf{k}}'_A + 7E_1 s_A^2 c'_A s'_A \hat{\mathbf{k}}_A\cdot\hat{\mathbf{k}}'_A + 2mc_A s_A c'^2_A - 2mc_A s_A s'^2_A + 4E_1 c_A s_A c'^2_A\\ & + E_1 c_A s_A s'^2_A - s_A^2 s'^2_A \mathbf{p}_1\cdot\hat{\mathbf{k}}_A\big] + 16i(\mathbf{n}\times\mathbf{p}_1)\cdot\hat{\mathbf{k}}'_A\big[4mc_A s_A s'^2_A\hat{\mathbf{k}}_A\cdot\hat{\mathbf{k}}'_A - 5E_1 c_A s_A s'^2_A \hat{\mathbf{k}}_A\cdot\hat{\mathbf{k}}'_A - 2mc_A^2 c'_A s'_A\\ & - 4E_1 c_A^2 c'_A s'_A - 5c_A s_A c'_A s'_A \mathbf{p}_1\cdot\hat{\mathbf{k}}_A - 2ms_A^2 c'_A s'_A - 3E_1 s_A^2 c'_A s'_A - s_A^2 s'^2_A \mathbf{p}_1\cdot\hat{\mathbf{k}}'_A + 2s_A^2 s'^2_A(\mathbf{p}_1\cdot\hat{\mathbf{k}}_A)(\hat{\mathbf{k}}_A\cdot\hat{\mathbf{k}}'_A)\big]\\ & + 16i(\mathbf{n}\times\hat{\mathbf{k}}_A)\cdot\hat{\mathbf{k}}'_A\big[4ms_A^2 c'_A s'_A \mathbf{p}_1\cdot\hat{\mathbf{k}}_A + 8m^2 c_A s_A c'_A s'_A + 4E_1 m s_A^2 s'^2_A \hat{\mathbf{k}}_A\cdot\hat{\mathbf{k}}'_A - s_A^2 s'^2_A(\mathbf{p}_1\cdot\mathbf{p}_1)(\hat{\mathbf{k}}_A\cdot\hat{\mathbf{k}}'_A)\\ & - 3E_1 c_A s_A s'^2_A \mathbf{p}_1\cdot\hat{\mathbf{k}}'_A - E_1 s_A^2 c'_A s'_A \mathbf{p}_1\cdot\hat{\mathbf{k}}_A - 3c_A s_A c'_A s'_A \mathbf{p}_1\cdot\mathbf{p}_1 - 8E_1^2 c_A s_A c'_A s'_A\big]\\ & + 16i(\mathbf{p}_1\times\hat{\mathbf{k}}_A)\cdot\hat{\mathbf{k}}'_A\big[s_A^2 s'^2_A(\mathbf{p}_1\cdot\hat{\mathbf{k}}_A)(\mathbf{n}\cdot\hat{\mathbf{k}}'_A) - s_A^2 s'^2_A(\mathbf{n}\cdot\hat{\mathbf{k}}_A)(\mathbf{p}_1\cdot\hat{\mathbf{k}}'_A)\\ & + s_A^2 s'^2_A(\mathbf{n}\cdot\mathbf{p}_1)(\hat{\mathbf{k}}_A\cdot\hat{\mathbf{k}}'_A) + 4mc_A s_A s'^2_A \mathbf{n}\cdot\hat{\mathbf{k}}'_A + E_1 s_A^2 c'_A s'_A \mathbf{n}\cdot\hat{\mathbf{k}}_A + 3E_1 c_A s_A s'^2_A \mathbf{n}\cdot\hat{\mathbf{k}}'_A + 3c_A s_A c'_A s'_A \mathbf{n}\cdot\mathbf{p}_1\big],\end{aligned} \tag{40}$$

where we denote the contracted trace part for $q_a q_b \to q_a q_b$ as $\mathrm{Tr}^2_{\mathrm{q_a q_b\to q_a q_b}}$, $c_A \equiv \cosh(\eta_{kA}/2)$, $c'_A \equiv \cosh(\eta'_{kA}/2)$, $s_A \equiv \sinh(\eta'_{kA}/2)$, and $s'_A \equiv \sinh(\eta'_{kA}/2)$. We see in (40) that there are four typical terms proportional to $(\mathbf{n}\times\mathbf{p}_1)\cdot\hat{\mathbf{k}}_A$, $(\mathbf{n}\times\mathbf{p}_1)\cdot\hat{\mathbf{k}}'_A$, $(\mathbf{n}\times\hat{\mathbf{k}}_A)\cdot\hat{\mathbf{k}}'_A$, and $(\mathbf{p}_1\times\hat{\mathbf{k}}_A)\cdot\hat{\mathbf{k}}'_A$, in which the first three terms are from the spin-orbit coupling and the last one corresponds to the noncoplanar part of $\mathbf{p}_1$, $\hat{\mathbf{k}}_A$, and $\hat{\mathbf{k}}'_A$. We will show in the next section that (40) is a good approximation for the contracted trace part to the exact result.

It can be proved that $\Delta I_M^{AB\to 12}$ for all 2-to-2 parton scatterings in Fig. 2 have the same structure as in (40) for $q_a q_b \to q_a q_b$ under the approximation in (38) and (39).

Note that $\Delta I_M^{AB\to 12}$ depends linearly on the direction of the scattering plane $\mathbf{n} = \hat{\mathbf{b}}\times\hat{\mathbf{p}}_A$, we can write the contracted trace part in the form of $\hat{\mathbf{b}}\cdot\mathbf{I}$, as is done in Eq. (23). We take the term $(\mathbf{n}\times\mathbf{p}_1)\cdot\hat{\mathbf{k}}_A$ in (40) as an example, which can be rewritten as

$$[(\hat{\mathbf{b}}\times\hat{\mathbf{p}}_A)\times\mathbf{p}_1]\cdot\hat{\mathbf{k}}_A = \hat{\mathbf{b}}\cdot[(\hat{\mathbf{p}}_A\cdot\hat{\mathbf{k}}_A)\mathbf{p}_1 - (\hat{\mathbf{p}}_A\cdot\mathbf{p}_1)\hat{\mathbf{k}}_A]. \tag{41}$$

Therefore $\mathbf{I}$ contains the term inside the square brackets on the right-hand side of Eq. (41). Another example is the term proportional to $(\mathbf{p}_1\times\hat{\mathbf{k}}_A)\cdot\hat{\mathbf{k}}'_A$: we see that all terms have factors of the form $\mathbf{n}\cdot\mathbf{V}$ ($\mathbf{V}=\hat{\mathbf{k}}_A, \hat{\mathbf{k}}'_A, \mathbf{p}_1$) inside the square brackets; these terms can be rewritten as $\mathbf{n}\cdot\mathbf{V} = \hat{\mathbf{b}}\cdot(\hat{\mathbf{p}}_A\times\mathbf{V})$, so $\mathbf{I}$ contains the term $\hat{\mathbf{p}}_A\times\mathbf{V}$.

VI. NUMERICAL METHOD TO CALCULATE QUARK/ANTIQUARK POLARIZATION RATE

In this section we will calculate the polarization rate for quarks in a QGP from Eq. (24). Here we assume a local equilibrium in particle momentum but not in spin. We will consider two cases: the approximation as in (38) and (39) and the exact result without any approximation. The main parameters are set to following values: the quark mass $m_q = 0.2$ GeV for quarks of all flavors ($u, d, s, \bar{u}, \bar{d}, \bar{s}$), the gluon mass $m_g = 0$ for the external gluon, the internal gluon mass (Debye screening mass) $m_g = m_D = 0.2$ GeV in gluon propagators in the t and u channel to regulate the possible divergence, the width $\alpha = 0.28$ GeV of the Gaussian wave packet, and the temperature $T = 0.3$ GeV.

Although the 2-to-2 processes for antiqaurk polarization are different from those for quarks, it can be shown that the polarization rate for antiquarks is the same as that for quarks, because all 2-to-2 scatterings for antiquark polarization can be obtained from those in Fig. 2 by making a particle-antiparticle transformation. In the following we discuss only the quark polarization. The same discussion can also be applied to the antiquark polarization.

The local polarization rate in Eq. (24) for quarks involves a 16-dimensional integration, which is a major challenge in the numerical calculation. In the Monte Carlo integration, the number of sample points grows exponentially with the dimension, so even a very rough calculation in high dimensions would need a huge number of sample points.

To overcome this difficulty, we split the integration into two parts: a ten-dimension (10D) integration over $(\mathbf{p}_{c,1}, \mathbf{p}_{c,2}, \mathbf{k}^T_{c,A}, \mathbf{k}'^T_{c,A})$ and a six-dimension (6D) integration over $(\mathbf{p}_A, \mathbf{p}_B)$. We carry out the 10D integration and store the result as a function of $\mathbf{p}_{c,A}$ (and $\mathbf{p}_{c,B} = -\mathbf{p}_{c,A}$). Then we carry out the 6D integration using the precalculated 10D integral.

The 10D integral, the last five lines of Eq. (24), depends on $\mathbf{p}_{c,A}$ and $\mathbf{p}_{c,B} = -\mathbf{p}_{c,A}$ which appear in the wave packet function ϕ_A and ϕ_B respectively. So we denote the 10D integral as $\Theta_{jk}(\mathbf{p}_{c,A})$, from Eq. (27) the polarization rate per unit volume for one quark flavor can be rewritten as

$$\frac{d^4\mathbf{P}_q(X)}{dX^4} = \frac{\pi}{(2\pi)^4}\frac{\partial(\beta u_\rho)}{\partial X^\nu}\sum_{A,B,1}\int\frac{d^3p_A}{(2\pi)^3 2E_A}\frac{d^3p_B}{(2\pi)^3 2E_B} \times |v_{c,A}-v_{c,B}|[\Lambda^{-1}]^\nu_{\ j}\mathbf{e}_{c,i}\epsilon_{ikh}\hat{\mathbf{p}}^h_{c,A} \times f_A(X,p_A)f_B(X,p_B)\big(p^\rho_A - p^\rho_B\big)\Theta_{jk}(\mathbf{p}_{c,A}) \equiv \frac{\partial(\beta u_\rho)}{\partial X^\nu}\mathbf{W}^{\rho\nu}, \tag{42}$$

where the second equality defines $\mathbf{W}^{\rho\nu}$ and the sum of $A, B, 1$ is over all 2-to-2 processes in Fig. 2.

A. 10D integration

The 10D integral $\Theta_{jk}(\mathbf{p}^{(z)}_{c,A})$ is calculated in the CMS by assuming $\mathbf{p}^{(z)}_{c,A} = (0,0,|\mathbf{p}_{c,A}|)$ and $\mathbf{p}^{(z)}_{c,B} = (0,0,-|\mathbf{p}_{c,A}|)$, where $|\mathbf{p}_{c,A}|$ is determined by the momenta of two incident particles in the laboratory frame as in Eq. (C1). We can obtain $\Theta_{jk}(\mathbf{p}_{c,A})$ by carrying out the rotation operation on the tensor $\Theta_{jk}(\mathbf{p}^{(z)}_{c,A})$ in accordance with the rotation matrix from $\mathbf{p}^{(z)}_{c,A}$ to $\mathbf{p}_{c,A}$.

For the Monte Carlo integration we have to sample $\mathbf{k}^T_{c,A}$, $\mathbf{k}'^T_{c,A}$, $\mathbf{p}_{c,1}$, and $\mathbf{p}_{c,2}$. First we sample $\mathbf{k}^T_{c,A}$ and $\mathbf{k}'^T_{c,A}$, where the main contribution comes from the Gaussian distribution (13). Here we draw samples of $\mathbf{k}^T_{c,A} = (k_{c,A,x}, k_{c,A,y}, 0)$ and $\mathbf{k}'^T_{c,A} = (k'_{c,A,x}, k'_{c,A,y}, 0)$ inside the 3σ ($\sigma = \alpha/\sqrt{2}$) region of the Gaussian distribution around the center point $\mathbf{p}^{(z)}_{c,A}$. The longitudinal momentum $k_{c,A,z}$ and $k'_{c,A,z}$ can be determined by the energy conservation once $\mathbf{p}_{c,1}$ and $\mathbf{p}_{c,2}$ are given.

Then we sample $\mathbf{p}_{c,1}$ and $\mathbf{p}_{c,2}$. In order to increase the efficiency of the sampling, we should determine the range of $\mathbf{p}_{c,1}$ and $\mathbf{p}_{c,2}$. We can first determine the ranges of lengths $|\mathbf{p}_{c,1}|$ and $|\mathbf{p}_{c,2}|$ by a numerical search. Then we determine the ranges of directions $\hat{\mathbf{p}}_{c,1}$ and $\hat{\mathbf{p}}_{c,2}$. For a given $\hat{\mathbf{p}}_{c,1}$, which can be randomly chosen, we find that the largest value of $\theta \equiv \arccos(-\hat{\mathbf{p}}_{c,1}\cdot\hat{\mathbf{p}}_{c,2})$ between $\hat{\mathbf{p}}_{c,2}$ and $-\hat{\mathbf{p}}_{c,1}$ occurs when

$$|\mathbf{k}_{c,A}| = |\mathbf{k}_{c,B}| = |\mathbf{p}_{c,1}| = |\mathbf{p}_{c,2}| = \sqrt{p^2_{c,A} + (3\sigma)^2}. \tag{43}$$

Hence we obtain the range of θ as

$$\theta \equiv \arccos(-\hat{\mathbf{p}}_{c,1}\cdot\hat{\mathbf{p}}_{c,2}) \in \left[0, \pi - 2\arccos\left(\frac{3\sigma}{\sqrt{p^2_{c,A}+(3\sigma)^2}}\right)\right]. \tag{44}$$

The azimuthal angle φ of $\hat{\mathbf{p}}_{c,2}$ around $-\hat{\mathbf{p}}_{c,1}$ is in the range $[0, 2\pi]$.

With the given values of $\mathbf{p}_{c,1}$ and $\mathbf{p}_{c,2}$, the values of $k_{c,A,z}$ and $k'_{c,A,z}$ can be obtained by solving Eq. (D9). Then $\mathbf{k}_{c,B}$ and $\mathbf{k}'_{c,B}$ can be determined by $\mathbf{k}_{c,B} = \mathbf{p}_{c,1} + \mathbf{p}_{c,2} - \mathbf{k}_{c,A}$ and $\mathbf{k}'_{c,B} = \mathbf{p}_{c,1} + \mathbf{p}_{c,2} - \mathbf{k}'_{c,A}$ respectively.

The 10D integral is done by ZMCintegral-3.0, a Monte Carlo integration package, that we have newly developed and runs on multi-GPUs [69]. The ZMCintegral package is able to evaluate 15^{10} sample points within a couple of hours depending on the complexity of the integrand. For our integrand with all 2-to-2 processes for quarks of all flavors and gluons, it takes about 5 h on one Tesla v100 card. We scan the values of $|\mathbf{p}_{c,A}|$ from 0.1 to 2.2 GeV and those of b_0 from 0.1 to 3.5 fm, then we store the integration results of $\Theta_{jk}(\mathbf{p}^{(z)}_{c,A})$ for later use. It takes a couple of days to finish the calculation. We find that when $|\mathbf{p}_{c,A}| > 2.5$ GeV, the 10D integral is almost zero. This is due to the fact that if $\alpha \ll |\mathbf{p}_{c,A}|$, the incident wave packets can be almost regarded as plane waves which give vanishing polarization.

B. 6D integration

Now we carry out the remaining 6D integration over $\mathbf{p}_A$ and $\mathbf{p}_B$ in (42). As we have mentioned in Sec. V that we assume partons with $p^\mu_A = (E_A, \mathbf{p}_A)$ and $p^\mu_B = (E_B, \mathbf{p}_B)$

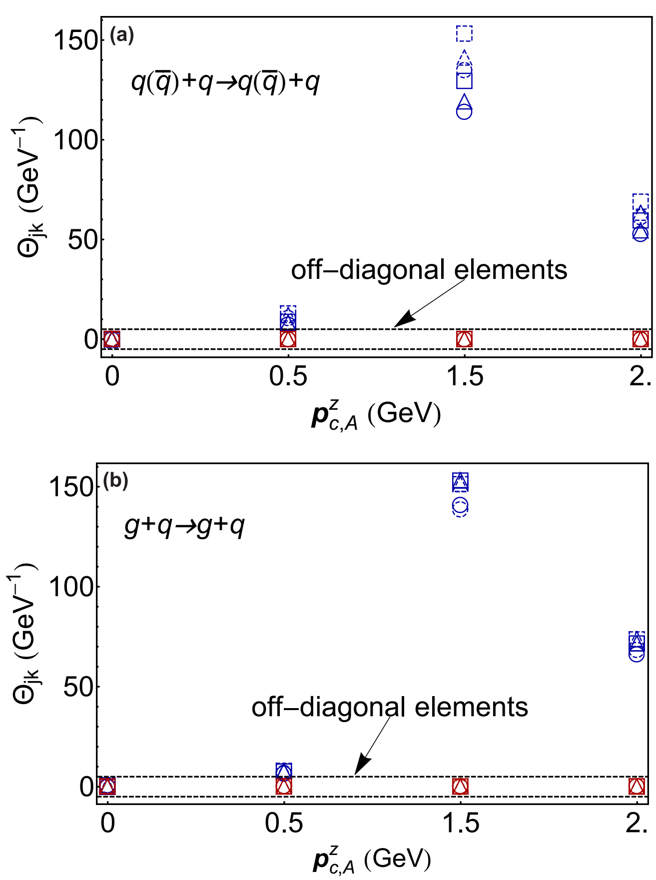

FIG. 3. Comparison of the results of the symmetric tensor $\Theta_{jk}(\mathbf{p}^{(z)}_{c,A})$ for (a) $q(\bar{q}) + q \to q(\bar{q}) + q$ and (b) $g + q \to g + q$ in two cases, with the approximation in (38) and (39) and exact calculation of the integral without any approximation. The unit of $\Theta_{jk}(\mathbf{p}^{(z)}_{c,A})$ is GeV^{-1}. The results for $g + g \to q + \bar{q}$ are not shown because they are negligibly small (almost zero). Here we choose $b_0 = 0.5$ fm and $|\mathbf{p}^{(z)}_{c,A}| = 0$, 0.5, 1.0, 1.5, 2.0 GeV. The solid symbols are the exact results without any approximation, while the dashed symbols are the results with approximation in (38) and (39). All off-diagonal elements are around zero and bounded inside two dashed lines: Θ_{12}, Θ_{13} and Θ_{23} are represented by circles, squares, and triangles in dark red, respectively. All diagonal elements are nonvanishing: Θ_{11}, Θ_{22}, and Θ_{33} are represented by circles, squares, and triangles in dark blue, respectively.

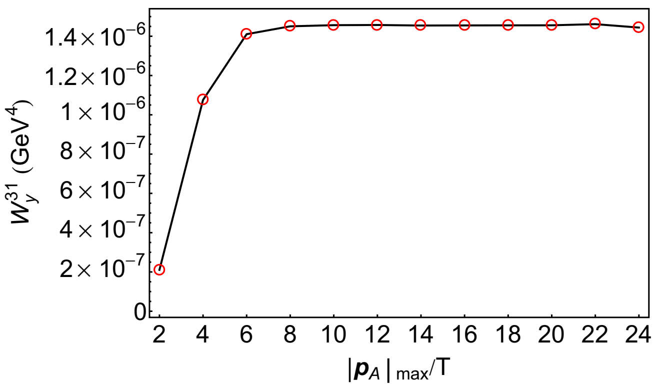

FIG. 4. The dependence of the results of $\mathbf{W}_y^{31}$ on the integral ranges $|\mathbf{p}_A|_{\max} = |\mathbf{p}_B|_{\max}$ for $q(\bar{q}) + q \rightarrow q(\bar{q}) + q$. We choose $b_0 = 2.2$ fm, $z = 0$ fm, $T = 0.3$ GeV.

in the laboratory frame follow the Boltzmann distribution, $f_i(X, p_i) = \exp[-\beta(X)p_i \cdot u(X)]$ for $i = A, B$.

The energy-momentum $p_{c,A}^{\mu} = (E_{c,A}, \mathbf{p}_{c,A})$ and $p_{c,B}^{\mu} = (E_{c,B}, \mathbf{p}_{c,B})$ in the CMS of two scattering particles are given by Eq. (C1), where the boost velocity and the Lorentz contraction factor are given by Eqs. (C2) and (C3) respectively. The impact parameter $\mathbf{b}_c$ in the CMS is given by Eq. (C7).

In the preceding subsection, we calculated the 10D integral $\Theta_{jk}(\mathbf{p}_{c,A}^{(z)})$ where $\mathbf{p}_{c,A}^{(z)}$ is in the z direction. We have to transform the tensor $\Theta_{jk}(\mathbf{p}_{c,A}^{(z)})$ to $\Theta_{jk}(\mathbf{p}_{c,A})$ so that $\mathbf{p}_{c,A}^{(z)}$ is rotated to the real direction of $\mathbf{p}_{c,A}$ determined by Eq. (C1). The rotation matrix R_{ij} is defined by $\mathbf{p}_{c,A,i} = R_{ij}\mathbf{p}_{c,A,j}^{(z)}$, with which we define the transformation for the tensor $\Theta_{jk}(\mathbf{p}_{c,A}) = R_{jj'}R_{kk'}\Theta_{j'k'}(\mathbf{p}_{c,A}^{(z)})$.

Our numerical results show that the tensor $\mathbf{W}^{\rho\nu}$ has the form

$$\mathbf{W}^{\rho\nu} = W\epsilon^{0\rho\nu j}\mathbf{e}_j, \tag{45}$$

where we see that ρ and ν should be spatial indices or $\mathbf{W}^{0\nu} = \mathbf{W}^{\rho 0} = \mathbf{0}$. The form of (45) will be verified in the numerical results in Sec. VII. Then from (42) we obtain the polarization rate per unit volume for one quark flavor,

$$\frac{d^4\mathbf{P}_q(X)}{dX^4} = \epsilon^{0j\rho\nu}\frac{\partial(\beta u_\rho)}{\partial X^\nu}W\mathbf{e}_j = 2\epsilon_{jkl}\omega_{kl}W\mathbf{e}_j$$
$$= 2W\nabla_X \times (\beta\mathbf{u}), \tag{46}$$

where $\omega_{\rho\nu} = -(1/2)[\partial_\rho^X(\beta u_\nu) - \partial_\nu^X(\beta u_\rho)]$, and for spatial indices we have the 3D form $\omega_{kl} = (1/2)[\nabla_k^X(\beta\mathbf{u}_l) - \nabla_l^X(\beta\mathbf{u}_k)]$ with $\mathbf{u}$ being the spatial part of the four-velocity u^ρ.

VII. NUMERICAL RESULTS

In this section we will present our numerical results. The approximation in (38) and (39) is inspired by the first order contribution in the narrow wave packet approximation. In order to see how effective the approximation is, we compare in Fig. 3 the results of the 10D integral $\Theta_{jk}(\mathbf{p}_{c,A}^{(z)})$ for the scattering processes $q(\bar{q}) + q \rightarrow q(\bar{q}) + q$ and $g + q \rightarrow g + q$ in two cases: with and without the approximation. Here the process $q(\bar{q}) + q \rightarrow q(\bar{q}) + q$ stands for a sum over five

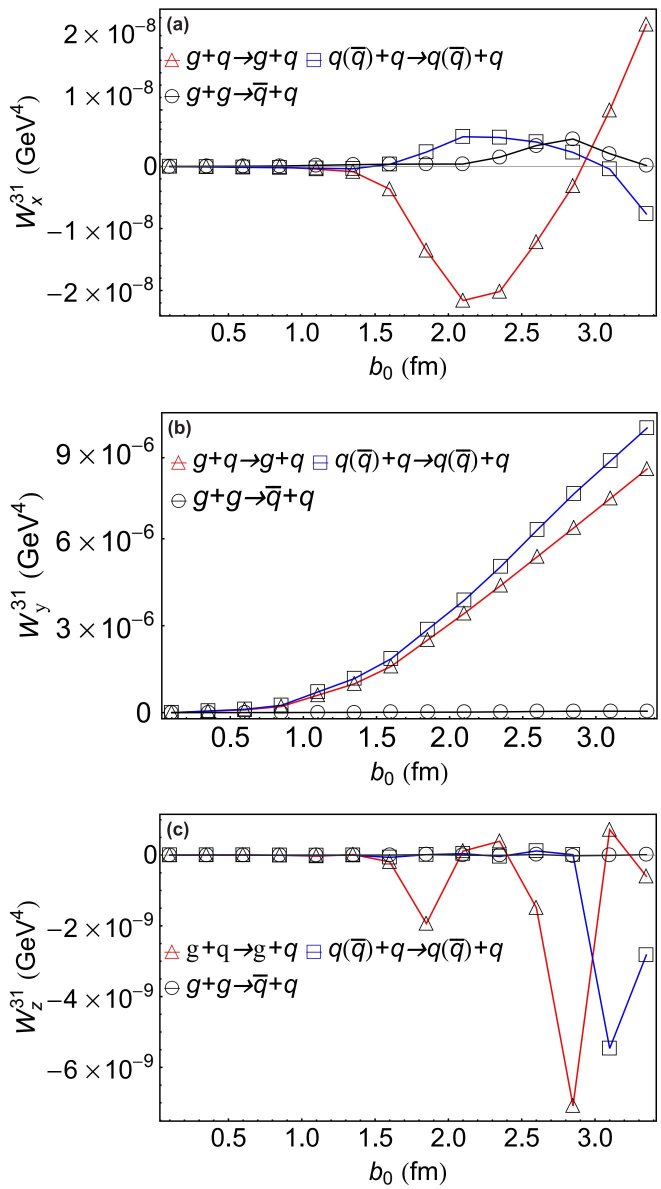

FIG. 5. Results for (a) $\mathbf{W}_x^{31}$, (b) $\mathbf{W}_y^{31}$, and (c) $\mathbf{W}_z^{31}$ as functions of the cutoff b_0 in fm. There are large fluctuations in $\mathbf{W}_x^{31}$ and $\mathbf{W}_z^{31}$ above $b_0 = 1.5$ fm due to the strong oscillation of Bessel functions.

different processes in Fig. 2. Note that we do not show the results for $g + g \rightarrow q + \bar{q}$ for which all elements of $\Theta_{jk}(\mathbf{p}_{c,A}^{(z)})$ are almost zero in contrast to processes with at least one incident quark. We see in the figure that the results with the approximation are in agreement with the exact ones in 20% precision. In the figure we see that all elements of $\Theta(\mathbf{p}_{c,A}^{(z)})$ fluctuate around zero for $|\mathbf{p}_{c,A}^{(z)}| = 0$, which leads to vanishing polarization. When $|\mathbf{p}_{c,A}^{(z)}|$ is nonvanishing, the off-diagonal elements of $\Theta(\mathbf{p}_{c,A}^{(z)})$ are still zero within errors, but all diagonal elements take positive values which are almost equal to each other.

We then work out the rest 6D integral and obtain $\mathbf{W}^{\rho\nu}$ in Eq. (45). In the 6D integration we have to determine the maximum value of $|\mathbf{p}_A|$ and $|\mathbf{p}_B|$ or the integration range of

$|\mathbf{p}_A|$ and $|\mathbf{p}_B|$. In Fig. 4, as an example, we show the dependence of $\mathbf{W}_y^{31}$ on $|\mathbf{p}_A|_{\max} = |\mathbf{p}_B|_{\max}$ for $q(\bar{q}) + q \to q(\bar{q}) + q$, where we choose $b_0 = 2.2$ fm, $z = 0$ fm, and $T = 0.3$ GeV. We see in the figure that the value of $\mathbf{W}_y^{31}$ is very stable when $|\mathbf{p}_A|_{\max} = |\mathbf{p}_B|_{\max} > 8T$.

The numerical results for $\mathbf{W}^{\rho\nu}$ show the structure of (45). We can write $\mathbf{W}^{\rho\nu}$ in an explicit matrix form,

$$\mathbf{W}^{\rho\nu} = \begin{pmatrix} 0 & 0 & 0 & 0 \\ 0 & 0 & W\mathbf{e}_z & -W\mathbf{e}_y \\ 0 & -W\mathbf{e}_z & 0 & W\mathbf{e}_x \\ 0 & W\mathbf{e}_y & -W\mathbf{e}_x & 0 \end{pmatrix}. \tag{47}$$

As an example, we show in Fig. 5 the results for all components of $\mathbf{W}^{31}$ as functions of the cutoff b_0 for the quark polarization. We see in the figure that $\mathbf{W}_x^{31}$ and $\mathbf{W}_z^{31}$ are two or three orders of magnitude smaller than the positive values of $\mathbf{W}_y^{31}$, which gives the polarization in the y direction. As we can see in the figure, $\mathbf{W}_y^{31}$ increases with the cutoff b_0. The reason for such a rising behavior is due to the Taylor expansion of $f_A(x_{c,A}, p_{c,A}) f_B(x_{c,B}, p_{c,B})$ to the linear order in $y_{c,T} = (0, \mathbf{b}_c)$ as in Appendix B. There should exist an upper limit for b_0 above which the coherence of the incident wave packets is broken and the results are not physical. Such an upper limit can be set to be the order of the hydrodynamical length scale $\sim 1/\partial_X^\mu u^\nu$ and should be larger than the interaction length scale $1/m_D$.

It can be proved that $\mathbf{W}^{31}$ for the antiquark polarization is the same as that for the quark one. The numerical results show that the magnitude of all elements $\mathbf{W}^{\rho\nu}$ are equal so we denote it as W.

VIII. DISCUSSIONS

We have constructed a microscopic model for the global polarization from particle scatterings in a many body system. The core of the idea is the scattering of particles as wave packets so that the orbital angular momentum is present in scatterings and can be converted to spin polarization. As an illustrative example, we have calculated the quark/antiquark polarization in a QGP. The quarks and gluons are assumed to obey the Boltzmann distribution which simplifies the heavy numerical calculation. There is no essential difficulty to treat quarks and gluons as fermions and bosons respectively.

To simplify the calculation, we also assume that the quark distributions are the same for all flavors and spin states. As a consequence, the inverse processes that one polarized quark is scattered by a parton to two final state partons as wave packets are absent. So the relaxation of polarization cannot be described without inverse processes and polarized distributions. We will extend our model by including the inverse processes in the future.

IX. SUMMARY AND CONCLUSIONS

The global polarization in heavy ion collisions arises from scattering processes of partons or hadrons with spin-orbit couplings. However, it is hard to implement this microscopic picture consistently to describe particle scatterings at specified impact parameters in a thermal medium with a shear flow. On the other hand the statistic-hydro model or Wigner function method are widely used to calculate the global polarization in heavy ion collisions. These models are based on the assumption that the spin degrees of freedom have reached a local equilibrium. So there should be a spin-vorticity coupling term in the distribution function to give the global polarization proportional to the vorticity when it is small. However it is unknown if particle spins are really in a local equilibrium. In this paper we aim to construct a microscopic model for the global polarization from particle collisions without the assumption of local equilibrium for spins. The polarization effect is incorporated into particle scatterings at specified impact parameters with spin-orbit couplings encoded. The spin-vorticity coupling naturally emerges from particle collisions if we assume a local equilibrium in particle momenta instead of particle spins. This provides a microscopic mechanism for the global polarization from the first principle through particle collisions in nonequilibrium.

As an illustrative example, we have calculated the quark polarization rate per unit volume from all 2-to-2 parton (quark or gluon) scatterings in a locally thermalized quark-gluon plasma in momentum. Although the processes for antiquark polarization are different from those for quarks, it can be shown that the polarization rate for antiquarks is the same as that for quarks because they are connected by the charge conjugate transformation. This is consistent with the fact that the rotation does not distinguish particles and antiparticles. The spin-orbit coupling is hidden in the polarized scattering amplitude at specified impact parameters. The polarization rate involves an integral of 16 dimensions, which is far beyond the capability of the current numerical algorithm. We have developed a new Monte Carlo integration algorithm ZMCintegral on multi-GPUs to make such a heavy task feasible. We have shown that the polarization rate per unit volume is proportional to the vorticity as the result of particle scatterings, a nonequilibrium scenario for the global polarization. So we can see in this example how the spin-vorticity coupling emerges naturally from particle scatterings.

ACKNOWLEDGMENTS

Q.W. thanks F. Becattini and M. Lisa for insightful discussions. Q.W. was supported in part by the National Natural Science Foundation of China (NSFC) under Grants No. 11535012 and No. 11890713, the 973 program under Grant No. 2015CB856902, and the Key Research Program of the Chinese Academy of Sciences under Grant No. XDPB09. X.N.W. was supported in part by the National Natural Science Foundation of China (NSFC) under Grants No. 11890714 and No. 11861131009, and by the Director, Office of Energy Research, Office of High Energy and Nuclear Physics, Division of Nuclear Physics, of the U.S. Department of Energy under Contract No. DE-AC02-05CH11231.

APPENDIX A: SINGLE PARTICLE STATE AS A WAVE PACKET IN RELATIVISTIC QUANTUM MECHANICS

In this Appendix, we will give definitions and conventions for the single particle state in coordinate and momentum space and those for the wave packet.

1. Single particle state in coordinate and momentum space

For simplicity we first consider the single particle state of spin-0 particles, then we generalize it to spin-1/2 particles.

A position eigenstate is denoted as $|\mathbf{x}\rangle$ and satisfies the following orthogonality and completeness conditions:

$$\langle \mathbf{x}'|\mathbf{x}\rangle = \delta^{(3)}(\mathbf{x}'-\mathbf{x}), \quad 1 = \int d^3x|\mathbf{x}\rangle\langle\mathbf{x}|. \tag{A1}$$

The normalization of the state $|\mathbf{x}\rangle$ is then

$$\langle \mathbf{x}|\mathbf{x}\rangle = \delta^{(3)}(\mathbf{x}-\mathbf{x}) = \int \frac{d^3p}{(2\pi)^3} = \frac{1}{\Omega}\sum_{\mathbf{p}}, \tag{A2}$$

where Ω is the space volume.

A momentum eigenstate is denoted as $|\mathbf{p}\rangle$ and satisfies the following orthogonality and completeness conditions:

$$\langle \mathbf{p}'|\mathbf{p}\rangle = 2E_p(2\pi)^3\delta^{(3)}(\mathbf{p}-\mathbf{p}'),$$
$$1 = \int \frac{d^3p}{(2\pi)^3}\frac{1}{2E_p}|\mathbf{p}\rangle\langle\mathbf{p}|, \tag{A3}$$

where $E_p = \sqrt{|\mathbf{p}|^2+m^2}$ is the energy of the particle. Note that $\langle \mathbf{p}'|\mathbf{p}\rangle$ is Lorentz invariant. The normalization of $|\mathbf{p}\rangle$ is then

$$\langle \mathbf{p}|\mathbf{p}\rangle = 2E_p(2\pi)^3\delta^{(3)}(\mathbf{p}-\mathbf{p}) = 2E_p\Omega. \tag{A4}$$

From Eqs. (A1) and (A3) we can define the inner product $\langle \mathbf{x}|\mathbf{p}\rangle$ as

$$\langle \mathbf{x}|\mathbf{p}\rangle = \sqrt{2E_p}e^{i\mathbf{p}\cdot\mathbf{x}}. \tag{A5}$$

With the above relation we can check that

$$\delta^{(3)}(\mathbf{x}-\mathbf{x}') = \langle \mathbf{x}'|\mathbf{x}\rangle = \int \frac{d^3p}{(2\pi)^3}\frac{1}{2E_p}\langle \mathbf{x}'|\mathbf{p}\rangle\langle\mathbf{p}|\mathbf{x}\rangle$$
$$= \int \frac{d^3p}{(2\pi)^3}e^{i\mathbf{p}\cdot(\mathbf{x}'-\mathbf{x})}, \tag{A6}$$

where we have inserted the completeness relation in (A3). We can express $|\mathbf{x}\rangle$ in terms of $|\mathbf{p}\rangle$ and vice versa,

$$|\mathbf{x}\rangle = \int \frac{d^3p}{(2\pi)^3}\frac{1}{2E_p}|\mathbf{p}\rangle\langle\mathbf{p}|\mathbf{x}\rangle = \int \frac{d^3p}{(2\pi)^3}\frac{1}{\sqrt{2E_p}}e^{-i\mathbf{p}\cdot\mathbf{x}}|\mathbf{p}\rangle,$$
$$|\mathbf{p}\rangle = \int d^3x|\mathbf{x}\rangle\langle\mathbf{x}|\mathbf{p}\rangle = \sqrt{2E_p}\int d^3x e^{i\mathbf{p}\cdot\mathbf{x}}|\mathbf{x}\rangle. \tag{A7}$$

2. Single particle state as a wave packet

In the real world a particle is always localized in some finite region, so its state can be represented by a wave packet $|\phi\rangle$ which is a superposition of plane wave states,

$$|\phi\rangle = \int \frac{d^3k}{(2\pi)^3}\frac{1}{\sqrt{2E_k}}\phi(\mathbf{k})|\mathbf{k}\rangle, \tag{A8}$$

and $\phi(\mathbf{k})$ is the amplitude and can be normalized to unity,

$$\langle \phi|\phi\rangle = \int \frac{d^3k}{(2\pi)^3}|\phi(\mathbf{k})|^2 = 1. \tag{A9}$$

The energy dimension of $|\phi\rangle$ is 0. A typical form for $\phi(\mathbf{p})$ satisfying Eq. (A9) is the Gaussian wave packet,

$$\phi(\mathbf{p}-\mathbf{p}_0) = \frac{(8\pi)^{3/4}}{\alpha^{3/2}}\exp\left[-\frac{(\mathbf{p}-\mathbf{p}_0)^2}{\alpha^2}\right], \tag{A10}$$

which is centered at $\mathbf{p}_0$. The wave-packet function in coordinate space is

$$\phi(\mathbf{x}) = \langle \mathbf{x}|\phi\rangle = \int \frac{d^3k}{(2\pi)^3}\phi(\mathbf{k})e^{i\mathbf{k}\cdot\mathbf{x}}, \tag{A11}$$

where we have used Eq. (A5).

If we displace the particle state by $\mathbf{b}$ in coordinate space, the new wave-packet function is given by

$$\phi'(\mathbf{x}) = \phi(\mathbf{x}-\mathbf{b}) = \int \frac{d^3k}{(2\pi)^3}\phi(\mathbf{k})e^{i\mathbf{k}\cdot(\mathbf{x}-\mathbf{b})} = \langle \mathbf{x}|\phi'\rangle, \tag{A12}$$

where the new wave-packet state is

$$|\phi'\rangle = \int \frac{d^3k}{(2\pi)^3}\frac{1}{\sqrt{2E_k}}\phi(\mathbf{k})e^{-i\mathbf{k}\cdot\mathbf{b}}|\mathbf{k}\rangle. \tag{A13}$$

For spin-1/2 particles, the single particle state $|\mathbf{k},\lambda\rangle$ has a spin index λ which is the spin along a quantization direction. The orthogonality and completeness conditions in (A3) now become

$$\langle \mathbf{k}',\lambda'|\mathbf{k},\lambda\rangle = 2E_k(2\pi)^3\delta^{(3)}(\mathbf{k}-\mathbf{k}')\delta_{\lambda,\lambda'},$$
$$1 = \int \frac{d^3p}{(2\pi)^3}\frac{1}{2E_p}\sum_{\lambda}|\mathbf{p},\lambda\rangle\langle\mathbf{p},\lambda|. \tag{A14}$$

The wave packet has the form

$$|\phi,\lambda\rangle = \int \frac{d^3k}{(2\pi)^3}\frac{1}{\sqrt{2E_k}}\phi(\mathbf{k})|\mathbf{k},\lambda\rangle, \tag{A15}$$

and satisfies the normalization condition $\langle\phi,\lambda|\phi,\lambda\rangle = 1$ similar to Eq. (A9).

APPENDIX B: EXPANSION OF f_A AND f_B IN IMPACT PARAMETER

We can make an expansion of $f_A(X_c+y_{c,T}/2, p_{c,A})$ $f_B(X_c-y_{c,T}/2, p_{c,B})$ in $y_{c,T}=(0,\mathbf{b}_c)$ if $|\mathbf{b}_c|$ is small compared with the range in which f_A and f_B change slowly. The variables with the subscript c are defined in the CMS of the scattering, while those without c are defined in the laboratory frame. We assume that the system has reached local equilibrium in momentum and the phase space distributions depend on the space-time through the fluid velocity $u^\mu(x)$ and temperature $T(x)$ in the form $f(x,p)=f[\beta(x)p\cdot u(x)]$.

To the linear order in $y_{c,T}$, we have

$$
\begin{aligned}
& f_A\left(X_c+\frac{y_{c,T}}{2}, p_{c,A}\right) f_B\left(X_c-\frac{y_{c,T}}{2}, p_{c,B}\right) \\
& \approx f_A(X_c, p_{c,A}) f_B(X_c, p_{c,B})+\frac{1}{2} y_{c,T}^{\mu}\left[\frac{\partial f_A(X_c, p_{c,A})}{\partial X_c^{\mu}} f_B(X_c, p_{c,B})-f_A(X_c, p_{c,A}) \frac{\partial f_B(X_c, p_{c,B})}{\partial X_c^{\mu}}\right] \\
& = f_A(X_c, p_{c,A}) f_B(X_c, p_{c,B})+\frac{1}{2} y_{c,T}^{\mu} \frac{\partial(\beta u_{c,\rho})}{\partial X_c^{\nu}}\left[p_{c,A}^{\rho} f_B(X_c, p_{c,B}) \frac{d f_A(X_c, p_{c,A})}{d(\beta u_c \cdot p_{c,A})}-p_{c,B}^{\rho} f_A(X_c, p_{c,A}) \frac{d f_B(X_c, p_{c,B})}{d(\beta u_c \cdot p_{c,B})}\right] \\
& = f_A(X, p_A) f_B(X, p_B)+\frac{1}{2} y_{c,T}^{\mu} \frac{\partial X^{\nu}}{\partial X_c^{\mu}} \frac{\partial(\beta u_{\rho})}{\partial X^{\nu}}\left[p_A^{\rho} f_B(X, p_B) \frac{d f_A(X, p_A)}{d(\beta u \cdot p_A)}-p_B^{\rho} f_A(X, p_A) \frac{d f_B(X, p_B)}{d(\beta u \cdot p_B)}\right],
\end{aligned} \tag{B1}
$$

where in the second equality we have boosted to the laboratory frame using $f_A(X, p_A) = f_A(X_c, p_{c,A})$ and $f_B(X, p_B) = f_B(X_c, p_{c,B})$. We look closely at the term $y_{c,T}^{\mu}[\partial(\beta u_{c,\rho})/\partial X_c^{\mu}]p_{c,A}^{\rho}$,

$$
\begin{aligned}
y_{c,T}^{\mu} p_{c,A}^{\rho} \frac{\partial(\beta u_{\rho})}{\partial X_c^{\mu}} & = \frac{1}{4} y_{c,T}^{[\mu} p_{c,A}^{\rho]}\left[\frac{\partial(\beta u_{c,\rho})}{\partial X_c^{\mu}}-\frac{\partial(\beta u_{c,\mu})}{\partial X_c^{\rho}}\right]+\frac{1}{4} y_{c,T}^{\{\mu} p_{c,A}^{\rho\}}\left[\frac{\partial(\beta u_{c,\rho})}{\partial X_c^{\mu}}+\frac{\partial(\beta u_{c,\mu})}{\partial X_c^{\rho}}\right] \\
& = -\frac{1}{2} y_{c,T}^{[\mu} p_{c,A}^{\rho]} \varpi_{\mu\rho}^{(c)}+\frac{1}{4} y_{c,T}^{\{\mu} p_{c,A}^{\rho\}}\left[\frac{\partial(\beta u_{c,\rho})}{\partial X_c^{\mu}}+\frac{\partial(\beta u_{c,\mu})}{\partial X_c^{\rho}}\right] \\
& = -\frac{1}{2} L_{(c)}^{\mu\rho} \varpi_{\mu\rho}^{(c)}+\frac{1}{4} y_{c,T}^{\{\mu} p_{c,A}^{\rho\}}\left[\frac{\partial(\beta u_{c,\rho})}{\partial X_c^{\mu}}+\frac{\partial(\beta u_{c,\mu})}{\partial X_c^{\rho}}\right],
\end{aligned} \tag{B2}
$$

where $[\mu\rho]$ and $\{\mu\rho\}$ denote the antisymmetrization and symmetrization of two indices respectively, $L_{(c)}^{\mu\rho} \equiv y_{c,T}^{[\mu} p_{c,A}^{\rho]}$ is the OAM tensor, and $\omega_{\mu\rho}^{(c)} \equiv -(1/2)[\partial_{\mu}^{X_c}(\beta u_{c,\rho}) - \partial_{\rho}^{X_c}(\beta u_{c,\mu})]$ is the thermal vorticity. We see that the coupling term of the OAM and vorticity appear in Eq. (B1). The second term in the last line of Eq. (B2) is related to the Killing condition required by the thermal equilibrium of the spin.

Using $X_c^{\mu} = \Lambda^{\mu}_{\ \nu} X^{\nu}$ and $X^{\mu} = [\Lambda^{-1}]^{\mu}_{\ \nu} X_c^{\nu}$, we have $\partial X^{\nu}/\partial X_c^{\mu} = [\Lambda^{-1}]^{\nu}_{\ \mu} = \Lambda_{\mu}^{\ \nu}$ and then Eq. (B1) becomes

$$
\begin{aligned}
& f_A\left(X_c+\frac{y_{c,T}}{2}, p_{c,A}\right) f_B\left(X_c-\frac{y_{c,T}}{2}, p_{c,B}\right) \\
& = f_A(X, p_A) f_B(X, p_B)+\frac{1}{2} y_{c,T}^{\mu}[\Lambda^{-1}]^{\nu}_{\ \mu} \frac{\partial(\beta u_{\rho})}{\partial X^{\nu}}\left[p_A^{\rho} f_B(X, p_B) \frac{d f_A(X, p_A)}{d(\beta u \cdot p_A)}-p_B^{\rho} f_A(X, p_A) \frac{d f_B(X, p_B)}{d(\beta u \cdot p_B)}\right].
\end{aligned} \tag{B3}
$$

In Appendix C we give the exact form of $\Lambda^{\mu}_{\ \nu}$ and $[\Lambda^{-1}]^{\mu}_{\ \nu}$.

APPENDIX C: LORENTZ TRANSFORMATION

In the laboratory frame two colliding particles have on-shell momenta $p_A = (E_A, \mathbf{p}_A)$ and $p_B = (E_B, \mathbf{p}_B)$. The Lorentz transformation for the energy momentum from the laboratory frame to the CMS of two colliding particles is

$$
\begin{aligned}
\mathbf{p}_{c,i} & = \mathbf{p}_i+(\gamma_{\rm bst}-1)\hat{\mathbf{v}}_{\rm bst}(\hat{\mathbf{v}}_{\rm bst}\cdot\mathbf{p}_i)-\gamma_{\rm bst}\mathbf{v}_{\rm bst}E_i, \\
E_{c,i} & = \gamma_{\rm bst}(E_i-\mathbf{v}_{\rm bst}\cdot\mathbf{p}_i),
\end{aligned} \tag{C1}
$$

where $i = A, B$, $\mathbf{v}_{\rm bst}$ is the boost velocity or the velocity of CMS in the laboratory frame and is given by

$$
\mathbf{v}_{\rm bst} = \frac{\mathbf{p}_A+\mathbf{p}_B}{E_A+E_B}, \tag{C2}
$$

and

$$
\gamma_{\rm bst} = (1-|\mathbf{v}_{\rm bst}|^2)^{-1/2} \tag{C3}
$$

is the Lorentz contraction factor corresponding to $\mathbf{v}_{\rm bst}$. Equation (C1) defines the Lorentz transformation matrix $\Lambda^{\mu}_{\ \nu}$. The reverse transformation to (C1) from the CMS to the laboratory frame can be obtained by flipping the sign of $\hat{\mathbf{v}}_{\rm bst}$,

$$
\begin{aligned}
\mathbf{p}_i & = \mathbf{p}_{c,i}+(\gamma_{\rm bst}-1)\hat{\mathbf{v}}_{\rm bst}(\hat{\mathbf{v}}_{\rm bst}\cdot\mathbf{p}_{c,i})+\gamma_{\rm bst}\mathbf{v}_{\rm bst}E_{c,i}, \\
E_i & = \gamma_{\rm bst}(E_{c,i}+\mathbf{v}_{\rm bst}\cdot\mathbf{p}_{c,i}).
\end{aligned} \tag{C4}
$$

The above defines the Lorentz transformation matrix $[\Lambda^{-1}]^{\mu}_{\ \nu}$.

The Lorentz transformation for $x_A = (t_A, \mathbf{x}_A)$ and $x_B = (t_B, \mathbf{x}_B)$ is

$$
\begin{aligned}
\mathbf{x}_{c,i} & = \mathbf{x}_i+(\gamma_{\rm bst}-1)\hat{\mathbf{v}}_{\rm bst}(\hat{\mathbf{v}}_{\rm bst}\cdot\mathbf{x}_i)-\gamma_{\rm bst}\mathbf{v}_{\rm bst}t_i, \\
t_{c,i} & = \gamma_{\rm bst}(t_i-\mathbf{v}_{\rm bst}\cdot\mathbf{x}_i).
\end{aligned} \tag{C5}
$$

The difference of two space-time points in the CMS are expressed in laboratory frame variables,

$$
\begin{aligned}
\Delta t_c & = t_{c,A}-t_{c,B} = \gamma_{\rm bst}(\Delta t-\mathbf{v}_{\rm bst}\cdot\Delta\mathbf{x}), \\
\Delta\mathbf{x}_c & = \Delta\mathbf{x}+(\gamma_{\rm bst}-1)\hat{\mathbf{v}}_{\rm bst}(\hat{\mathbf{v}}_{\rm bst}\cdot\Delta\mathbf{x})-\gamma_{\rm bst}\mathbf{v}_{\rm bst}\Delta t,
\end{aligned} \tag{C6}
$$

where $\Delta t = t_A - t_B$ and $\Delta\mathbf{x} = \mathbf{x}_A - \mathbf{x}_B$. We then express the impact parameter as

$$
\mathbf{b}_c = \Delta\mathbf{x}_c\cdot(1-\hat{\mathbf{p}}_{c,A}\hat{\mathbf{p}}_{c,A}). \tag{C7}
$$

Let us look at the CMS constraint $\delta(\Delta t_c)\delta(\Delta x_{c,L})$ in Eq. (10) (we have recovered the subscript c). The condition $\Delta t_c = 0$ leads to

$$\Delta t = \mathbf{v}_{\rm bst} \cdot \Delta\mathbf{x}, \tag{C8}$$

while the condition $\hat{\mathbf{p}}_{c,A} \cdot \Delta\mathbf{x}_c = 0$ leads to

$$(\mathbf{v}_A - \mathbf{v}_B) \cdot \Delta\mathbf{x} = 0, \tag{C9}$$

where we have used

$$\Delta\mathbf{x}_c = \Delta\mathbf{x} + \left(\gamma_{\rm bst}^{-1} - 1\right)\hat{\mathbf{v}}_{\rm bst}(\hat{\mathbf{v}}_{\rm bst} \cdot \Delta\mathbf{x}), \tag{C10}$$

which is the result of Eqs. (C6) and (C8). The condition in Eq. (C9) means that $(\mathbf{x}_A - \mathbf{x}_B) \perp (\mathbf{v}_A - \mathbf{v}_B)$. Equations (C8) and (C9) are the laboratory frame version of the constraint $\delta(\Delta t_c)\delta(\Delta x_{c,L})$.

APPENDIX D: INTEGRATION OVER IMPACT PARAMETER AND DELTA FUNCTIONS IN EQ. (21)

We carry out the integration over the impact parameter and show how to remove the delta functions by integration in Eq. (21).

Substituting Eq. (23) into Eq. (21), we have the integration of $\mathbf{b}_c$ in the following form:

$$\begin{aligned} I(\mathbf{b}_c) &= i\int d^2\mathbf{b}_c \exp\left(i\mathbf{a}\cdot\mathbf{b}_c\right)\frac{1}{b_c^2}\mathbf{b}_{c,j}\mathbf{b}_{c,k}\mathbf{b}_{c,l} \\ &= -\frac{\partial}{\partial\mathbf{a}_l}\frac{\partial}{\partial\mathbf{a}_j}\frac{\partial}{\partial\mathbf{a}_k}\int d^2\mathbf{b}_c \exp\left(i\mathbf{a}\cdot\mathbf{b}_c\right)\frac{1}{b_c^2} \\ &= -2\pi\frac{\partial}{\partial\mathbf{a}_l}\frac{\partial}{\partial\mathbf{a}_j}\frac{\partial}{\partial\mathbf{a}_k}\int_0^{b_0} db_c\frac{1}{b_c}J_0(ab_c), \end{aligned} \tag{D1}$$

where $b_c \equiv |\mathbf{b}_c|$, b_0 is the cutoff of b_c, $\mathbf{a} = \mathbf{k}'_{c,A} - \mathbf{k}_{c,A}$, and

$$J_0(ab_c) = \frac{1}{2\pi}\int_0^{2\pi} d\phi \exp\left(iab_c\cos\phi\right). \tag{D2}$$

Then we carry out the derivatives on $\mathbf{a}_j$, $\mathbf{a}_k$, and $\mathbf{a}_l$,

$$\begin{aligned} I(\mathbf{b}_c) = &-2\pi\frac{1}{a^3}Q_{jkl}^L\int_0^{w_0} dw w^2 J_0'''(w) \\ &-2\pi\frac{1}{a^3}Q_{jkl}^T\int_0^{w_0} dw[wJ_0''(w) + J_1(w)], \end{aligned} \tag{D3}$$

where we have used $w_0 = ab_0$ with b_0 being the upper limit or cutoff of b_c, J_i $(i = 0, 1, 2)$ are Bessel functions, and

$$\begin{aligned} Q_{jkl}^L &= \frac{\mathbf{a}_l\mathbf{a}_j\mathbf{a}_k}{a^3}, \\ Q_{jkl}^T &= \frac{1}{a^3}(a^2\mathbf{a}_k\delta_{lj} + a^2\mathbf{a}_l\delta_{jk} + a^2\mathbf{a}_j\delta_{lk} - 3\mathbf{a}_l\mathbf{a}_j\mathbf{a}_k). \end{aligned} \tag{D4}$$

Note that the overall minus sign of Eq. (D3) cancels the one in Eq. (21).

We carry out the integration to remove the delta functions. First we integrate over $\mathbf{k}_{c,B}$ and $\mathbf{k}'_{c,B}$ to remove six delta functions in three momenta; the result is to make the following replacement in the integrand,

$$\begin{aligned} \mathbf{k}_{c,B} &= \mathbf{p}_{c,1} + \mathbf{p}_{c,2} - \mathbf{k}_{c,A}, \\ \mathbf{k}'_{c,B} &= \mathbf{p}_{c,1} + \mathbf{p}_{c,2} - \mathbf{k}'_{c,A}. \end{aligned} \tag{D5}$$

We are left with two delta functions for energy conservation which can be removed by the integration over $k_{c,A}^L$ and $k_{c,A}'^L$, where L means the longitudinal direction along $\mathbf{p}_{c,A}$. To this purpose, we express the energies in terms of longitudinal and transverse momenta

$$\begin{aligned} E_{c,A} &= \sqrt{\left(k_{c,A}^L\right)^2 + \left(\mathbf{k}_{c,A}^T\right)^2 + m^2}, \\ E_{c,B} &= \sqrt{\left(\mathbf{p}_{c,1}^T + \mathbf{p}_{c,2}^T - \mathbf{k}_{c,A}^T\right)^2 + \left(p_{c,1}^L + p_{c,2}^L - k_{c,A}^L\right)^2 + m^2}, \\ E'_{c,A} &= \sqrt{\left(k_{c,A}'^L\right)^2 + \left(\mathbf{k}_{c,A}'^T\right)^2 + m^2}, \\ E'_{c,B} &= \sqrt{\left(\mathbf{p}_{c,1}^T + \mathbf{p}_{c,2}^T - \mathbf{k}_{c,A}'^T\right)^2 + \left(p_{c,1}^L + p_{c,2}^L - k_{c,A}'^L\right)^2 + m^2}. \end{aligned} \tag{D6}$$

So two delta functions for energy conservation become

$$\begin{aligned} I(\delta E) &= \delta(E_{c,A} + E_{c,B} - E_{c,1} - E_{c,2}) \\ &= \frac{1}{\left|\mathrm{Ja}\left[k_{c,A}^L(1)\right]\right|}\delta\left[k_{c,A}^L - k_{c,A}^L(1)\right] \\ &\quad + \frac{1}{\left|\mathrm{Ja}\left[k_{c,A}^L(2)\right]\right|}\delta\left[k_{c,A}^L - k_{c,A}^L(2)\right] \\ I(\delta E') &= \delta(E'_{c,A} + E'_{c,B} - E_{c,1} - E_{c,2}) \\ &= \frac{1}{\left|\mathrm{Ja}\left[k_{c,A}'^L(1)\right]\right|}\delta\left[k_{c,A}'^L - k_{c,A}'^L(1)\right] \\ &\quad + \frac{1}{\left|\mathrm{Ja}\left[k_{c,A}'^L(2)\right]\right|}\delta\left[k_{c,A}'^L - k_{c,A}'^L(2)\right] \end{aligned} \tag{D7}$$

where the Jacobians of two delta functions are given by

$$\begin{aligned} \mathrm{Ja}\left(k_{c,A}^L\right) &= \frac{\partial}{\partial k_{c,A}^L}(E_{c,A} + E_{c,B} - E_{c,1} - E_{c,2}) \\ &= k_{c,A}^L\left(\frac{1}{E_{c,A}} + \frac{1}{E_{c,B}}\right) - \frac{1}{E_{c,B}}\left(p_{c,1}^L + p_{c,2}^L\right), \\ \mathrm{Ja}\left(k_{c,A}'^L\right) &= \frac{\partial}{\partial k_{c,A}'^L}(E'_{c,A} + E'_{c,B} - E_{c,1} - E_{c,2}) \\ &= k_{c,A}'^L\left(\frac{1}{E'_{c,A}} + \frac{1}{E'_{c,B}}\right) - \frac{1}{E'_{c,B}}\left(p_{c,1}^L + p_{c,2}^L\right), \end{aligned} \tag{D8}$$

and $k_{c,A}^L(i = 1, 2)$ and $k_{c,A}'^L(i = 1, 2)$ are two roots of the energy conservation equation $E_{c,A} + E_{c,B} - E_{c,1} - E_{c,2} = 0$ and $E'_{c,A} + E'_{c,B} - E_{c,1} - E_{c,2} = 0$, respectively. The explicit forms of $k_{c,A}^L(i = 1, 2)$ and $k_{c,A}'^L(i = 1, 2)$ are

$$\begin{aligned} k_{c,A}^L(1, 2) &= C_1 \pm C_2, \\ k_{c,A}'^L(1, 2) &= k_{c,A}^L(1, 2)\left[\mathbf{k}_{c,A}^T \to \mathbf{k}_{c,A}'^T\right], \end{aligned} \tag{D9}$$

where C_1 and C_2 are given by

$$C_1 = \frac{1}{2}\cdot\frac{p^L_{c,1}+p^L_{c,2}}{(E_{c,1}+E_{c,2})^2-\left(p^L_{c,1}+p^L_{c,2}\right)^2}\times\left[(E_{c,1}+E_{c,2})^2-\left(p^L_{c,1}+p^L_{c,2}\right)^2+2\left(\mathbf{p}^T_{c,1}+\mathbf{p}^T_{c,2}\right)\cdot\mathbf{k}^T_{c,A}-\left(\mathbf{p}^T_{c,1}+\mathbf{p}^T_{c,2}\right)^2\right],$$
$$C_2 = -\frac{1}{2}\cdot\frac{E_{c,1}+E_{c,2}}{(E_{c,1}+E_{c,2})^2-\left(p^L_{c,1}+p^L_{c,2}\right)^2}\sqrt{H}, \quad \text{(D10)}$$

with H being defined by

$$H = (E_{c,1}+E_{c,2})^4+4m^2\left(p^L_{c,1}+p^L_{c,2}\right)^2+(\mathbf{p}_{c,1}+\mathbf{p}_{c,2})^4+4\left(\mathbf{k}^T_{c,A}\right)^2(\mathbf{p}_{c,1}+\mathbf{p}_{c,2})^2-4(\mathbf{p}_{c,1}+\mathbf{p}_{c,2})^2\times\left[\mathbf{k}^T_{c,A}\cdot\left(\mathbf{p}^T_{c,1}+\mathbf{p}^T_{c,2}\right)\right]-2(E_{c,1}+E_{c,2})^2\times\left[2m^2+2\left(\mathbf{k}^T_{c,A}\right)^2-2\mathbf{k}^T_{c,A}\cdot\left(\mathbf{p}^T_{c,1}+\mathbf{p}^T_{c,2}\right)+(\mathbf{p}_{c,1}+\mathbf{p}_{c,2})^2\right]. \quad \text{(D11)}$$

APPENDIX E: SOME FORMULA FOR DIRAC SPINORS

The Hamiltonian for a Dirac fermion with the mass m is given by

$$H = \boldsymbol{\alpha}\cdot\mathbf{p}+\gamma_0 m = \begin{pmatrix} m & \boldsymbol{\sigma}\cdot\mathbf{p} \\ \boldsymbol{\sigma}\cdot\mathbf{p} & -m \end{pmatrix}, \quad \text{(E1)}$$

where $\gamma^\mu = (\gamma_0, \boldsymbol{\gamma})$ are Dirac gamma matrices, $\boldsymbol{\alpha}\equiv\gamma_0\boldsymbol{\gamma}$, and $\boldsymbol{\sigma} = (\sigma_1, \sigma_2, \sigma_3)$ are Pauli matrices. The energy eigenstate can be found from the equation

$$H\begin{pmatrix}\chi\\ \phi\end{pmatrix} = \pm E_p\begin{pmatrix}\chi\\ \phi\end{pmatrix}, \quad \text{(E2)}$$

where $E_p = \sqrt{\mathbf{p}^2+m^2}$, the sign $\pm$ on the right-hand side corresponds to the positive/negative energy state, χ and ϕ are Pauli spinors which form a Dirac spinor (χ, ϕ). We can express χ in terms of ϕ and vice versa,

$$\chi = \frac{\boldsymbol{\sigma}\cdot\mathbf{p}}{\eta E_p - m}\phi,$$
$$\phi = \frac{\boldsymbol{\sigma}\cdot\mathbf{p}}{\eta E_p + m}\chi, \quad \text{(E3)}$$

where $\eta = \pm 1$ correspond to the positive and negative energy state respectively. So the positive energy solution becomes

$$u(s,\mathbf{p}) = \sqrt{E_p+m}\begin{pmatrix}\chi_s\\ \frac{\boldsymbol{\sigma}\cdot\mathbf{p}}{E_p+m}\chi_s\end{pmatrix}, \quad \text{(E4)}$$

where $s = \pm 1$ is the spin orientation of the Pauli spinor and $\mathbf{n} = (\sin\theta\cos\phi, \sin\theta\sin\phi, \cos\theta)$ is the spin quantization direction. The spin eigenstates along $\mathbf{n}$ are given by

$$\chi_+ = \begin{pmatrix} e^{-i\phi}\cos\frac{\theta}{2}\\ \sin\frac{\theta}{2}\end{pmatrix},$$
$$\chi_- = \begin{pmatrix} -e^{-i\phi}\sin\frac{\theta}{2}\\ \cos\frac{\theta}{2}\end{pmatrix}, \quad \text{(E5)}$$

which satisfy

$$\sigma\cdot\mathbf{n} = \begin{pmatrix}\cos\theta & e^{-i\phi}\sin\theta\\ e^{i\phi}\sin\theta & -\cos\theta\end{pmatrix},$$
$$(\sigma\cdot\mathbf{n})\chi_s = s\chi_s. \quad \text{(E6)}$$

The negative energy solution can be put into the form

$$\tilde{v}(s,\mathbf{p}) = \sqrt{E_p+m}\begin{pmatrix}-\frac{\boldsymbol{\sigma}\cdot\mathbf{p}}{E_p+m}\chi_s\\ \chi_s\end{pmatrix}. \quad \text{(E7)}$$

The Dirac spinor for antiparticles can be defined by

$$v(s,\mathbf{p}) = \tilde{v}(-s,-\mathbf{p}) = \sqrt{E_p+m}\begin{pmatrix}\frac{\boldsymbol{\sigma}\cdot\mathbf{p}}{E_p+m}\chi_{-s}\\ \chi_{-s}\end{pmatrix}, \quad \text{(E8)}$$

or defined in terms of the positive energy solution,

$$v(s,\mathbf{p}) = i\gamma^2 u^*(s,\mathbf{p}) = -i\sqrt{E_p+m}\begin{pmatrix}\frac{\boldsymbol{\sigma}\cdot\mathbf{p}}{E_p+m}\sigma_2\chi^*_s\\ \sigma_2\chi^*_s\end{pmatrix}. \quad \text{(E9)}$$

The two Dirac spinors in (E8) and (E9) are actually the same up to a sign.

Now we rewrite the Dirac spinor of a moving particle in the way of a Lorentz transformation of the one in the particle's rest frame. The Lorentz transformation matrix for the Dirac spinor is given by

$$\Lambda_{1/2}(\mathbf{p}) = \exp\left(-\tfrac{1}{2}\eta_p\boldsymbol{\alpha}\cdot\hat{\mathbf{p}}\right) = \cosh\left(\tfrac{1}{2}\eta_p\right)-(\boldsymbol{\alpha}\cdot\hat{\mathbf{p}})\sinh\left(\tfrac{1}{2}\eta_p\right),$$
$$\Lambda^{-1}_{1/2}(\mathbf{p}) = \Lambda_{1/2}(-\mathbf{p}) = \exp\left(\tfrac{1}{2}\eta_p\boldsymbol{\alpha}\cdot\hat{\mathbf{p}}\right), \quad \text{(E10)}$$

where $\hat{\mathbf{p}}\equiv\mathbf{p}/|\mathbf{p}|$ is the momentum direction, η_p is the rapidity satisfying $E_p = m\cosh(\eta_p)$, $|\mathbf{p}| = m\sinh(\eta_p)$, $v_p = \tanh(\eta_p)$, $E_p+m = 2m\cosh^2(\frac{1}{2}\eta_p)$, $E_p-m = 2m\sinh^2(\frac{1}{2}\eta_p)$. So $u(s,\mathbf{p})$ can be expressed by a Lorentz boost of $u(s,\mathbf{0})$ for the particle at rest,

$$u(s,\mathbf{p}) = \sqrt{E_p+m}\begin{pmatrix}\chi_s\\ \frac{\boldsymbol{\sigma}\cdot\mathbf{p}}{E_p+m}\chi_s\end{pmatrix} = \Lambda_{1/2}(-\mathbf{p})u(s,\mathbf{0}) = \sqrt{2m}\begin{pmatrix}\cosh\left(\frac{1}{2}\eta_p\right)\chi_s\\ (\boldsymbol{\sigma}\cdot\hat{\mathbf{p}})\sinh\left(\frac{1}{2}\eta_p\right)\chi_s\end{pmatrix}. \quad \text{(E11)}$$

In the same way we can rewrite $v(s,\mathbf{p})$ as

$$v(s,\mathbf{p}) = \sqrt{E_p+m}\begin{pmatrix}\frac{\boldsymbol{\sigma}\cdot\mathbf{p}}{E_p+m}\chi_{-s}\\ \chi_{-s}\end{pmatrix} = \Lambda_{1/2}(-\mathbf{p})v(s,\mathbf{0}) = \sqrt{2m}\begin{pmatrix}(\boldsymbol{\sigma}\cdot\hat{\mathbf{p}})\sinh\left(\frac{1}{2}\eta_p\right)\chi_{-s}\\ \cosh\left(\frac{1}{2}\eta_p\right)\chi_{-s}\end{pmatrix}. \quad \text{(E12)}$$

With Eqs. (E11) and (E12) we have following formula:

$$\sum_s u(s,\mathbf{p})\bar{u}(s,\mathbf{q}) = \Lambda_{1/2}(-\mathbf{p})\left[\sum_s u(s,\mathbf{0})\bar{u}(s,\mathbf{0})\right]\Lambda^{-1}_{1/2}(-\mathbf{q}) = m\Lambda_{1/2}(-\mathbf{p})(1+\gamma_0)\Lambda^{-1}_{1/2}(-\mathbf{q}),$$
$$\sum_s v(s,\mathbf{p})\bar{v}(s,\mathbf{q}) = \Lambda_{1/2}(-\mathbf{p})\left[\sum_s v(s,\mathbf{0})\bar{v}(s,\mathbf{0})\right]\Lambda^{-1}_{1/2}(-\mathbf{q}) = m\Lambda_{1/2}(-\mathbf{p})(\gamma_0-1)\Lambda^{-1}_{1/2}(-\mathbf{q}), \quad \text{(E13)}$$

where we have used $\bar{u}(s,\mathbf{q})=\bar{u}(s,\mathbf{0})\Lambda_{1/2}^{-1}(-\mathbf{q})$, $\bar{v}(s,\mathbf{q})=\bar{v}(s,\mathbf{0})\Lambda_{1/2}^{-1}(-\mathbf{q})$, $\sum_s u(s,\mathbf{0})\bar{u}(s,\mathbf{0})=m(1+\gamma_0)$, and $\sum_s v(s,\mathbf{0})\bar{v}(s,\mathbf{0})=m(-1+\gamma_0)$.

The spin projector is defined by

$$\Pi(s,n)=\tfrac{1}{2}(1+s\gamma_5 n^\sigma\gamma_\sigma), \tag{E14}$$

where n^σ is the Lorentz boost of the polarization vector $(0,\mathbf{n})$ in the particle's rest frame satisfying $n\cdot p=0$ and $n^2=-1$. In the particle's rest frame, we have

$$\begin{aligned}\Pi_{\text{rest}}(s,n)&=\frac{1}{2}(1+s\mathbf{n}\cdot\mathbf{\Sigma})\\&\equiv\frac{1}{2}\begin{pmatrix}1+s\mathbf{n}\cdot\boldsymbol{\sigma} & 0\\ 0 & 1-s\mathbf{n}\cdot\boldsymbol{\sigma}\end{pmatrix}.\end{aligned} \tag{E15}$$

We have the following properties for the spin projector:

$$\begin{aligned}\Pi(s,n)u(s,\mathbf{p})&=u(s,\mathbf{p}),\\ \Pi(s,n)v(s,\mathbf{p})&=v(s,\mathbf{p}),\\ \Pi(s,n)u(-s,\mathbf{p})&=0,\\ \Pi(s,n)v(-s,\mathbf{p})&=0.\end{aligned} \tag{E16}$$

As an example, we can explicitly verify the first one as

$$\begin{aligned}\Pi(s,n)u(s,\mathbf{p})&=\tfrac{1}{2}\Lambda_{1/2}(-\mathbf{p})u(s,\mathbf{0})+\tfrac{1}{2}sn^\sigma\gamma_5\Lambda_{1/2}(-\mathbf{p})\\&\quad\times\Lambda_{1/2}^{-1}(-\mathbf{p})\gamma_\sigma\Lambda_{1/2}(-\mathbf{p})u(s,\mathbf{0})\\&=\tfrac{1}{2}\Lambda_{1/2}(-\mathbf{p})u(s,\mathbf{0})\\&\quad+\tfrac{1}{2}s\Lambda_{1/2}(-\mathbf{p})\gamma_5 n^\sigma\Lambda_\sigma^{\ \nu}(-\mathbf{p})\gamma_\nu u(s,\mathbf{0})\\&=\tfrac{1}{2}\Lambda_{1/2}(-\mathbf{p})u(s,\mathbf{0})\\&\quad+\tfrac{1}{2}s\Lambda_{1/2}(-\mathbf{p})\gamma_0(\mathbf{n}\cdot\mathbf{\Sigma})u(s,\mathbf{0})\\&=\Lambda_{1/2}(-\mathbf{p})\Pi_{\text{rest}}(s,n)u(s,\mathbf{0})\\&=u(s,\mathbf{p}),\end{aligned} \tag{E17}$$

where we have used $\Lambda_{1/2}^{-1}(-\mathbf{p})\gamma_\sigma\Lambda_{1/2}(-\mathbf{p})=\Lambda_\sigma^{\ \nu}(-\mathbf{p})\gamma_\nu$ and $\Lambda_\sigma^{\ \nu}(-\mathbf{p})=\Lambda^\nu_{\ \sigma}(\mathbf{p})$. Using the spin projector, we have the following relation:

$$\begin{aligned}&\Pi(s_0,n)\sum_s u(s,\mathbf{p})\bar{u}(s,\mathbf{p})\\&=\Pi(s_0,n)(p\cdot\gamma+m)|_{p^\mu=(E_p,\mathbf{p})}\\&=u(s_0,\mathbf{p})\bar{u}(s_0,\mathbf{p}),\end{aligned} \tag{E18}$$

where $p\cdot\gamma\equiv p_\mu\gamma^\mu$.

APPENDIX F: POLARIZED AMPLITUDES FOR QUARKS IN 2-TO-2 PARTON SCATTERINGS

In this Appendix, we give polarized amplitudes for quarks in all 2-to-2 parton scatterings listed in Fig. 2. We assume the same quark mass m for all flavors and that the external gluon is massless. We introduce a mass into internal gluons or gluon propagators in the t and u channels to regulate the possible divergence.

All kinematic variables are defined in the CMS in this Appendix; for notational simplicity we will suppress the subscript c for all variables—for example, p_A actually means p_{cA}. The values of color factors, denoted as $C_{AB\to CD}$ for the process $A+B\to C+D$, are given in Table I.

1. $q_aq_b\to q_aq_b$ with $a\neq b$

Following the Feynman diagram in Fig. 2, we obtain the difference in the squared amplitude between the spin state $s_2=1/2$ and $s_2=-1/2$ for q_b in the final state,

$$\begin{aligned}\Delta I_M^{q_aq_b\to q_aq_b}&=I_M^{q_aq_b\to q_aq_b}(s_2=1/2)-I_M^{q_aq_b\to q_aq_b}(s_2=-1/2)\\&=C_{q_aq_b\to q_aq_b}g_s^4m^2\frac{1}{q^2q'^2}\mathrm{Tr}\big[(p_1\cdot\gamma+m)\gamma^\mu\Lambda_{1/2}(-\mathbf{k}_A)(\gamma_0+1)\Lambda_{1/2}^{-1}(-\mathbf{k}'_A)\gamma^\nu\big]\\&\quad\times\mathrm{Tr}\big[\gamma_5(n\cdot\gamma)(p_2\cdot\gamma+m)\gamma_\mu\Lambda_{1/2}(-\mathbf{k}_B)(\gamma_0+1)\Lambda_{1/2}^{-1}(-\mathbf{k}'_B)\gamma_\nu\big],\end{aligned} \tag{F1}$$

where $q=k_A-p_1$ and $q'=k'_A-p_1$ are momenta in the propagators.

2. $\bar{q}_aq_b\to\bar{q}_aq_b$ with $a\neq b$

For the polarization of q_b, we obtain

$$\begin{aligned}\Delta I_M^{\bar{q}_aq_b\to\bar{q}_aq_b}&=C_{\bar{q}_aq_b\to\bar{q}_aq_b}g_s^4m^2\frac{1}{q^2q'^2}\mathrm{Tr}\big[\gamma^\mu(p_1\cdot\gamma-m)\gamma^\nu\Lambda_{1/2}(-\mathbf{k}'_A)(\gamma_0-1)\Lambda_{1/2}^{-1}(-\mathbf{k}_A)\big]\\&\quad\times\mathrm{Tr}\big[\gamma_5(n\cdot\gamma)(p_2\cdot\gamma+m)\gamma_\mu\Lambda_{1/2}(-\mathbf{k}_B)(\gamma_0+1)\Lambda_{1/2}^{-1}(-\mathbf{k}'_B)\gamma_\nu\big],\end{aligned} \tag{F2}$$

where $q=k_A-p_1$ and $q'=k'_A-p_1$ are momenta in the propagators.

3. $\bar{q}_a q_a \to \bar{q}_a q_a$

For the polarization of q_a in the final state, we obtain

$$
\begin{aligned}
\Delta I_M^{\bar{q}_a q_a \to \bar{q}_a q_a} = {} & C^{(1)}_{\bar{q}_a q_a \to \bar{q}_a q_a} g_s^4 m^2 \frac{1}{q_1^2 q_1'^2} \mathrm{Tr}\big[\gamma_5 (n\cdot\gamma)(p_2\cdot\gamma + m)\gamma^\mu \Lambda_{1/2}(-\mathbf{k}_B)(\gamma_0+1)\Lambda^{-1}_{1/2}(-\mathbf{k}'_B)\gamma^\nu\big] \\
& \times \mathrm{Tr}\big[(p_1\cdot\gamma - m)\gamma_\nu \Lambda_{1/2}(-\mathbf{k}'_A)(\gamma_0-1)\Lambda^{-1}_{1/2}(-\mathbf{k}_A)\gamma_\mu\big] \\
& - C^{(2)}_{\bar{q}_a q_a \to \bar{q}_a q_a} g_s^4 m^2 \frac{1}{q_1^2 q_2'^2} \mathrm{Tr}\big[\gamma_5 (n\cdot\gamma)(p_2\cdot\gamma + m)\gamma^\mu \Lambda_{1/2}(-\mathbf{k}_B)(\gamma_0+1)\Lambda^{-1}_{1/2}(-\mathbf{k}'_B)\gamma^\nu \\
& \times \Lambda_{1/2}(-\mathbf{k}'_A)(\gamma_0-1)\Lambda^{-1}_{1/2}(-\mathbf{k}_A)\gamma_\mu (p_1\cdot\gamma - m)\gamma_\nu\big] \\
& - C^{(2)}_{\bar{q}_a q_a \to \bar{q}_a q_a} g_s^4 m^2 \frac{1}{q_2^2 q_1'^2} \mathrm{Tr}\big[\gamma_5 (n\cdot\gamma)(p_2\cdot\gamma + m)\gamma_\mu (p_1\cdot\gamma - m)\gamma_\nu \\
& \times \Lambda_{1/2}(-\mathbf{k}'_A)(\gamma_0-1)\Lambda^{-1}_{1/2}(-\mathbf{k}_A)\gamma^\mu \Lambda_{1/2}(-\mathbf{k}_B)(\gamma_0+1)\Lambda^{-1}_{1/2}(-\mathbf{k}'_B)\gamma^\nu\big] \\
& + C^{(1)}_{\bar{q}_a q_a \to \bar{q}_a q_a} g_s^4 m^2 \frac{1}{q_2^2 q_2'^2} \mathrm{Tr}\big[\Lambda_{1/2}(-\mathbf{k}'_A)(\gamma_0-1)\Lambda^{-1}_{1/2}(-\mathbf{k}_A)\gamma^\mu \Lambda_{1/2}(-\mathbf{k}_B)(\gamma_0+1)\Lambda^{-1}_{1/2}(-\mathbf{k}'_B)\gamma^\nu\big] \\
& \times \mathrm{Tr}[\gamma_5 (n\cdot\gamma)(p_2\cdot\gamma + m)\gamma_\mu (p_1\cdot\gamma - m)\gamma_\nu],
\end{aligned} \tag{F3}
$$

where $q_1 = k_A - p_1$, $q_2 = k_A + k_B$, $q'_1 = k'_A - p_1$, and $q'_2 = k'_A + k'_B$ are momenta in the propagators.

4. $q_a q_a \to q_a q_a$

For the polarization of q_a in the final state, we obtain

$$
\begin{aligned}
\Delta I_M^{q_a q_a \to q_a q_a} = {} & C^{(1)}_{q_a q_a \to q_a q_a} g_s^4 m^2 \frac{1}{q_1^2 q_1'^2} \mathrm{Tr}\big[(p_1\cdot\gamma + m)\gamma^\mu \Lambda_{1/2}(-\mathbf{k}_A)(\gamma_0+1)\Lambda^{-1}_{1/2}(-\mathbf{k}'_A)\gamma^\nu\big] \\
& \times \mathrm{Tr}\big[\gamma_5 (n\cdot\gamma)(p_2\cdot\gamma + m)\gamma_\mu \Lambda_{1/2}(-\mathbf{k}_B)(\gamma_0+1)\Lambda^{-1}_{1/2}(-\mathbf{k}'_B)\gamma_\nu\big] \\
& - C^{(2)}_{q_a q_a \to q_a q_a} g_s^4 m^2 \frac{1}{q_1^2 q_2'^2} \mathrm{Tr}\big[(p_1\cdot\gamma + m)\gamma^\mu \Lambda_{1/2}(-\mathbf{k}_A)(\gamma_0+1)\Lambda^{-1}_{1/2}(-\mathbf{k}'_A)\gamma^\nu \\
& \times \gamma_5 (n\cdot\gamma)(p_2\cdot\gamma + m)\gamma_\mu \Lambda_{1/2}(-\mathbf{k}_B)(\gamma_0+1)\Lambda^{-1}_{1/2}(-\mathbf{k}'_B)\gamma_\nu\big] \\
& - C^{(2)}_{q_a q_a \to q_a q_a} g_s^4 m^2 \frac{1}{q_1'^2 q_2^2} \mathrm{Tr}\big[\gamma^\mu \Lambda_{1/2}(-\mathbf{k}_A)(\gamma_0+1)\Lambda^{-1}_{1/2}(-\mathbf{k}'_A)\gamma^\nu (p_1\cdot\gamma + m) \\
& \times \gamma_\mu \Lambda_{1/2}(-\mathbf{k}_B)(\gamma_0+1)\Lambda^{-1}_{1/2}(-\mathbf{k}'_B)\gamma_\nu \gamma_5 (n\cdot\gamma)(p_2\cdot\gamma + m)\big] \\
& + C^{(1)}_{q_a q_a \to q_a q_a} g_s^4 m^2 \frac{1}{q_2'^2 q_2^2} \mathrm{Tr}\big[\gamma_5 (n\cdot\gamma)(p_2\cdot\gamma + m)\gamma^\mu \Lambda_{1/2}(-\mathbf{k}_A)(\gamma_0+1)\Lambda^{-1}_{1/2}(-\mathbf{k}'_A)\gamma^\nu\big] \\
& \times \mathrm{Tr}\big[\Lambda_{1/2}(-\mathbf{k}_B)(\gamma_0+1)\Lambda^{-1}_{1/2}(-\mathbf{k}'_B)\gamma_\nu (p_1\cdot\gamma + m)\gamma_\mu\big],
\end{aligned} \tag{F4}
$$

where $q_1 = k_A - p_1$, $q_2 = k_A - p_2$, $q'_1 = k'_A - p_1$, and $q'_2 = k'_A - p_2$ are momenta in propagators.

5. $gg \to \bar{q}_a q_a$

In principle, the ghost diagrams should also contribute. However, its contribution is canceled when we calculate $\Delta I_M^{gg\to\bar{q}_a q_a}$. For the polarization of q_a in the final state, we obtain

$$
\begin{aligned}
\Delta I_M^{gg\to\bar{q}_a q_a} = {} & C^{(1)}_{gg\to\bar{q}_a q_a} g_s^4 \frac{1}{(q_1^2 - m^2)(q_1'^2 - m^2)} I_1 + C^{(2)}_{gg\to\bar{q}_a q_a} g_s^4 \frac{1}{(q_1^2 - m^2)(q_2'^2 - m^2)} I_2 \\
& - C^{(3)}_{gg\to\bar{q}_a q_a} g_s^4 \frac{1}{(q_1^2 - m^2) q_3'^2} I_3 + C^{(2)}_{gg\to\bar{q}_a q_a} g_s^4 \frac{1}{(q_1'^2 - m^2)(q_2^2 - m^2)} I_4 \\
& + C^{(1)}_{gg\to\bar{q}_a q_a} g_s^4 \frac{1}{(q_2^2 - m^2)(q_2'^2 - m^2)} I_5 + C^{(3)}_{gg\to\bar{q}_a q_a} g_s^4 \frac{1}{(q_2^2 - m^2) q_3'^2} I_6 \\
& - C^{(3)}_{gg\to\bar{q}_a q_a} g_s^4 \frac{1}{(q_1'^2 - m^2) q_3^2} I_7 + C^{(3)}_{gg\to\bar{q}_a q_a} g_s^4 \frac{1}{(q_2'^2 - m^2) q_3^2} I_8 + C^{(4)}_{gg\to\bar{q}_a q_a} g_s^4 \frac{1}{q_3^2 q_3'^2} I_9,
\end{aligned} \tag{F5}
$$

where $q_1 = k_A - p_1$, $q_2 = p_2 - k_A$, $q_3 = k_A + k_B$, $q_1' = k_A' - p_1$, $q_2' = p_2 - k_A'$, and $q_3' = k_A' + k_B'$ are momenta in propagators, and the terms I_i for $i = 1, 2, \ldots, 9$ are given by

$$I_1 = \mathrm{Tr}[\gamma_5(n\cdot\gamma)(p_2\cdot\gamma+m)\gamma^{\nu}(q_1\cdot\gamma+m)\gamma^{\mu}(p_1\cdot\gamma-m)\gamma^{\mu'}(q_1'\cdot\gamma+m)\gamma^{\nu'}]g_{\mu\mu'}g_{\nu\nu'}, \tag{F6}$$

$$I_2 = \mathrm{Tr}[\gamma_5(n\cdot\gamma)(p_2\cdot\gamma+m)\gamma^{\nu}(q_1\cdot\gamma+m)\gamma^{\mu}(p_1\cdot\gamma-m)\gamma^{\nu'}(q_2'\cdot\gamma+m)\gamma^{\mu'}]g_{\mu\mu'}g_{\nu\nu'}, \tag{F7}$$

$$I_3 = \mathrm{Tr}[\gamma_5(n\cdot\gamma)(p_2\cdot\gamma+m)\gamma^{\nu}(q_1\cdot\gamma+m)\gamma^{\mu}(p_1\cdot\gamma-m)\gamma_{\sigma'}]g_{\mu\mu'}g_{\nu\nu'} \times[g^{\sigma'\mu'}(-q_3'-k_A')^{\nu'}+g^{\mu'\nu'}(k_A'-k_B')^{\sigma'}+g^{\nu'\sigma'}(k_B'+q_3')^{\mu'}], \tag{F8}$$

$$I_4 = \mathrm{Tr}[\gamma_5(n\cdot\gamma)(p_2\cdot\gamma+m)\gamma^{\mu}(q_2\cdot\gamma+m)\gamma^{\nu}(p_1\cdot\gamma-m)\gamma^{\mu'}(q_1'\cdot\gamma+m)\gamma^{\nu'}]g_{\mu\mu'}g_{\nu\nu'}, \tag{F9}$$

$$I_5 = \mathrm{Tr}[\gamma_5(n\cdot\gamma)(p_2\cdot\gamma+m)\gamma^{\mu}(q_2\cdot\gamma+m)\gamma^{\nu}(p_1\cdot\gamma-m)\gamma^{\nu'}(q_2'\cdot\gamma+m)\gamma^{\mu'}]g_{\mu\mu'}g_{\nu\nu'}, \tag{F10}$$

$$I_6 = \mathrm{Tr}[\gamma_5(n\cdot\gamma)(p_2\cdot\gamma+m)\gamma^{\mu}(q_2\cdot\gamma+m)\gamma^{\nu}(p_1\cdot\gamma-m)\gamma_{\sigma'}]g_{\mu\mu'}g_{\nu\nu'} \times[g^{\sigma'\mu'}(-q_3'-k_A')^{\nu'}+g^{\mu'\nu'}(k_A'-k_B')^{\sigma'}+g^{\nu'\sigma'}(k_B'+q_3')^{\mu'}], \tag{F11}$$

$$I_7 = \mathrm{Tr}[\gamma_5(n\cdot\gamma)(p_2\cdot\gamma+m)\gamma_{\sigma}(p_1\cdot\gamma-m)\gamma^{\mu'}(q_1'\cdot\gamma+m)\gamma^{\nu'}]g_{\mu\mu'}g_{\nu\nu'} \times[g^{\sigma\mu}(-q_3-k_A)^{\nu}+g^{\mu\nu}(k_A-k_B)^{\sigma}+g^{\nu\sigma}(k_B+q_3)^{\mu}], \tag{F12}$$

$$I_8 = \mathrm{Tr}[\gamma_5(n\cdot\gamma)(p_2\cdot\gamma+m)\gamma_{\sigma}(p_1\cdot\gamma-m)\gamma^{\nu'}(q_2'\cdot\gamma+m)\gamma^{\mu'}]g_{\mu\mu'}g_{\nu\nu'} \times[g^{\sigma\mu}(-q_3-k_A)^{\nu}+g^{\mu\nu}(k_A-k_B)^{\sigma}+g^{\nu\sigma}(k_B+q_3)^{\mu}], \tag{F13}$$

$$I_9 = \mathrm{Tr}[\gamma_5(n\cdot\gamma)(p_2\cdot\gamma+m)\gamma_{\sigma}(p_1\cdot\gamma-m)\gamma_{\sigma'}][g^{\sigma\mu}(-q_3-k_A)^{\nu}+g^{\mu\nu}(k_A-k_B)^{\sigma}+g^{\nu\sigma}(k_B+q_3)^{\mu}] \times[g^{\sigma'\mu'}(-q_3'-k_A')^{\nu'}+g^{\mu'\nu'}(k_A'-k_B')^{\sigma'}+g^{\nu'\sigma'}(k_B'+q_3')^{\mu'}]g_{\mu\mu'}g_{\nu\nu'}. \tag{F14}$$

6. $gq_a \to gq_a$

In principle, the ghost diagram should also contribute. However, its contribution is canceled when we calculate $\Delta I_M^{gq_a\to gq_a}$. For the polarization of q_a in the final state, we obtain

$$\begin{aligned}\Delta I_M^{gq_a\to gq_a} ={}& C^{(1)}_{gq_a\to gq_a}g_s^4 m\frac{1}{q_1^2q_1'^2}I_1 + C^{(2)}_{gq_a\to gq_a}g_s^4 m\frac{1}{q_1^2(q_2'^2-m^2)}I_2 - C^{(2)}_{gq_a\to gq_a}g_s^4 m\frac{1}{q_1^2(q_3'^2-m^2)}I_3\\ &+C^{(2)}_{gq_a\to gq_a}g_s^4 m\frac{1}{q_1'^2(q_2^2-m^2)}I_4 + C^{(3)}_{gq_a\to gq_a}g_s^4 m\frac{1}{(q_2^2-m^2)(q_2'^2-m^2)}I_5 + C^{(4)}_{gq_a\to gq_a}g_s^4 m\frac{1}{(q_2^2-m^2)(q_3'^2-m^2)}I_6\\ &-C^{(2)}_{gq_a\to gq_a}g_s^4 m\frac{1}{q_1'^2(q_3^2-m^2)}I_7 + C^{(4)}_{gq_a\to gq_a}g_s^4 m\frac{1}{(q_2'^2-m^2)(q_3^2-m^2)}I_8 + C^{(3)}_{gq_a\to gq_a}g_s^4 m\frac{1}{(q_3^2-m^2)(q_3'^2-m^2)}I_9,\end{aligned} \tag{F15}$$

where $q_1 = k_A - p_1$, $q_2 = p_2 - k_A$, $q_3 = k_A + k_B$, $q_1' = k_A' - p_1$, $q_2' = p_2 - k_A'$, and $q_3' = k_A' + k_B'$ are momenta in propagators, and the terms I_i for $i = 1, 2, \ldots, 9$ are given by

$$\begin{aligned}I_1 ={}& \mathrm{Tr}\big[\gamma_5(n\cdot\gamma)(p_2\cdot\gamma+m)\gamma_{\sigma}\Lambda_{1/2}(-\mathbf{k}_B)(\gamma_0+1)\Lambda^{-1}_{1/2}(-\mathbf{k}_B')\gamma_{\sigma'}\big]\\ &\times g_{\mu\mu'}g_{\nu\nu'}[g^{\mu\nu}(k_A+p_1)^{\sigma}+g^{\nu\sigma}(q_1-p_1)^{\mu}+g^{\sigma\mu}(-q_1-k_A)^{\nu}]\\ &\times[g^{\mu'\nu'}(k_A'+p_1)^{\sigma'}+g^{\nu'\sigma'}(q_1'-p_1)^{\mu'}+g^{\sigma'\mu'}(-q_1'-k_A')^{\nu'}],\end{aligned} \tag{F16}$$

$$I_2 = \mathrm{Tr}\big[\gamma_5(n\cdot\gamma)(p_2\cdot\gamma+m)\gamma_{\sigma}\Lambda_{1/2}(-\mathbf{k}_B)(\gamma_0+1)\Lambda^{-1}_{1/2}(-\mathbf{k}_B')\gamma^{\nu'}(q_2'\cdot\gamma+m)\gamma^{\mu'}\big]g_{\mu\mu'}g_{\nu\nu'} \times[g^{\mu\nu}(k_A+p_1)^{\sigma}+g^{\nu\sigma}(q_1-p_1)^{\mu}+g^{\sigma\mu}(-q_1-k_A)^{\nu}], \tag{F17}$$

$$I_3 = \mathrm{Tr}\big[\gamma_5(n\cdot\gamma)(p_2\cdot\gamma+m)\gamma_{\sigma}\Lambda_{1/2}(-\mathbf{k}_B)(\gamma_0+1)\Lambda^{-1}_{1/2}(-\mathbf{k}_B')\gamma^{\mu'}(q_3'\cdot\gamma+m)\gamma^{\nu'}\big]g_{\mu\mu'}g_{\nu\nu'} \times[g^{\mu\nu}(k_A+p_1)^{\sigma}+g^{\nu\sigma}(q_1-p_1)^{\mu}+g^{\sigma\mu}(-q_1-k_A)^{\nu}], \tag{F18}$$

$$I_4 = \mathrm{Tr}\big[\gamma_5(n\cdot\gamma)(p_2\cdot\gamma+m)\gamma^{\mu}(q_2\cdot\gamma+m)\gamma^{\nu}\Lambda_{1/2}(-\mathbf{k}_B)(\gamma_0+1)\Lambda^{-1}_{1/2}(-\mathbf{k}_B')\gamma_{\sigma'}\big]g_{\mu\mu'}g_{\nu\nu'} \times[g^{\mu'\nu'}(k_A'+p_1)^{\sigma'}+g^{\nu'\sigma'}(q_1'-p_1)^{\mu'}+g^{\sigma'\mu'}(-q_1'-k_A')^{\nu'}], \tag{F19}$$

$$I_5 = \mathrm{Tr}\big[\gamma_5(n\cdot\gamma)(p_2\cdot\gamma+m)\gamma^{\mu}(q_2\cdot\gamma+m)\gamma^{\nu}\Lambda_{1/2}(-\mathbf{k}_B)(\gamma_0+1)\Lambda^{-1}_{1/2}(-\mathbf{k}_B')\gamma^{\nu'}(q_2'+m)\gamma^{\mu'}\big]g_{\mu\mu'}g_{\nu\nu'}, \tag{F20}$$

$$I_6 = \mathrm{Tr}\big[\gamma_5(n\cdot\gamma)(p_2\cdot\gamma+m)\gamma^{\mu}(q_2\cdot\gamma+m)\gamma^{\nu}\Lambda_{1/2}(-\mathbf{k}_B)(\gamma_0+1)\Lambda^{-1}_{1/2}(-\mathbf{k}_B')\gamma^{\mu'}(q_3'\cdot\gamma+m)\gamma^{\nu'}\big]g_{\mu\mu'}g_{\nu\nu'}, \tag{F21}$$

$$I_7 = \mathrm{Tr}\big[\gamma_5(n\cdot\gamma)(p_2\cdot\gamma+m)\gamma^{\nu}(q_3\cdot\gamma+m)\gamma^{\mu}\Lambda_{1/2}(-\mathbf{k}_B)(\gamma_0+1)\Lambda_{1/2}^{-1}(-\mathbf{k}'_B)\gamma_{\sigma'}\big]g_{\mu\mu'}g_{\nu\nu'}$$
$$\times[g^{\mu'\nu'}(k'_A+p_1)^{\sigma'}+g^{\nu'\sigma'}(q'_1-p_1)^{\mu'}+g^{\sigma'\mu'}(-q'_1-k'_A)^{\nu'}], \quad \text{(F22)}$$

$$I_8 = \mathrm{Tr}\big[\gamma_5(n\cdot\gamma)(p_2\cdot\gamma+m)\gamma^{\nu}(q_3\cdot\gamma+m)\gamma^{\mu}\Lambda_{1/2}(-\mathbf{k}_B)(\gamma_0+1)\Lambda_{1/2}^{-1}(-\mathbf{k}'_B)\gamma^{\nu'}(q'_2\cdot\gamma+m)\gamma^{\mu'}\big]g_{\mu\mu'}g_{\nu\nu'}, \quad \text{(F23)}$$

$$I_9 = \mathrm{Tr}\big[\gamma_5(n\cdot\gamma)(p_2\cdot\gamma+m)\gamma^{\nu}(q_3\cdot\gamma+m)\gamma^{\mu}\Lambda_{1/2}(-\mathbf{k}_B)(\gamma_0+1)\Lambda_{1/2}^{-1}(-\mathbf{k}'_B)\gamma^{\mu'}(q'_3\cdot\gamma+m)\gamma^{\nu'}\big]g_{\mu\mu'}g_{\nu\nu'}. \quad \text{(F24)}$$

7. $\bar{q}_a q_a \rightarrow \bar{q}_b q_b$ with $a \neq b$

For the polarization of q_b in the final state, we obtain

$$\Delta I_M^{\bar{q}_a q_a\rightarrow\bar{q}_b q_b} = C_{\bar{q}_a q_a\rightarrow\bar{q}_b q_b}g_s^4 m^2\frac{1}{q^2q'^2}\mathrm{Tr}\big[\Lambda_{1/2}(-\mathbf{k}'_A)(\gamma_0-1)\Lambda_{1/2}^{-1}(-\mathbf{k}_A)\gamma^{\mu}\Lambda_{1/2}(-\mathbf{k}_B)(\gamma_0+1)\Lambda_{1/2}^{-1}(-\mathbf{k}'_B)\gamma^{\nu}\big]$$
$$\times\mathrm{Tr}[\gamma_5(n\cdot\gamma)(p_2\cdot\gamma-m)\gamma_{\mu}(p_1\cdot\gamma-m)\gamma_{\nu}], \quad \text{(F25)}$$

where $q = k_A + k_B$ and $q' = k'_A + k'_B$ are momenta in propagators.

[1] Z.-T. Liang and X.-N. Wang, Phys. Rev. Lett. **94**, 102301 (2005); **96**, 039901(E) (2006).
[2] Z.-T. Liang and X.-N. Wang, Phys. Lett. B **629**, 20 (2005).
[3] S. A. Voloshin, arXiv:nucl-th/0410089.
[4] B. Betz, M. Gyulassy, and G. Torrieri, Phys. Rev. C **76**, 044901 (2007).
[5] F. Becattini, F. Piccinini, and J. Rizzo, Phys. Rev. C **77**, 024906 (2008).
[6] J.-H. Gao, S.-W. Chen, W.-t. Deng, Z.-T. Liang, Q. Wang, and X.-N. Wang, Phys. Rev. C **77**, 044902 (2008).
[7] Q. Wang, Nucl. Phys. A **967**, 225 (2017).
[8] X.-G. Huang, P. Huovinen, and X.-N. Wang, Phys. Rev. C **84**, 054910 (2011).
[9] L. Adamczyk *et al.* (STAR Collaboration), Nature (London) **548**, 62 (2017).
[10] J. Adam *et al.* (STAR Collaboration), Phys. Rev. C **98**, 014910 (2018).
[11] T. Niida (STAR Collaboration), Nucl. Phys. A **982**, 511 (2019).
[12] F. Becattini, V. Chandra, L. Del Zanna, and E. Grossi, Ann. Phys. **338**, 32 (2013).
[13] F. Becattini and E. Grossi, Phys. Rev. D **92**, 045037 (2015).
[14] F. Becattini, I. Karpenko, M. A. Lisa, I. Upsal, and S. A. Voloshin, Phys. Rev. C **95**, 054902 (2017).
[15] W. Florkowski, B. Friman, A. Jaiswal, and E. Speranza, Phys. Rev. C **97**, 041901(R) (2018).
[16] W. Florkowski, B. Friman, A. Jaiswal, R. Ryblewski, and E. Speranza, Phys. Rev. D **97**, 116017 (2018).
[17] W. Florkowski, A. Kumar, and R. Ryblewski, Phys. Rev. C **98**, 044906 (2018).
[18] W. Florkowski, R. Ryblewski, and A. Kumar, Prog. Part. Nucl. Phys. **108**, 103709 (2019).
[19] U. W. Heinz, Phys. Rev. Lett. **51**, 351 (1983).
[20] H.-T. Elze, M. Gyulassy, and D. Vasak, Nucl. Phys. B **276**, 706 (1986).
[21] D. Vasak, M. Gyulassy, and H.-T. Elze, Ann. Phys. **173**, 462 (1987).
[22] P. Zhuang and U. W. Heinz, Ann. Phys. **245**, 311 (1996).
[23] W. Florkowski, J. Hufner, S. P. Klevansky, and L. Neise, Ann. Phys. **245**, 445 (1996).
[24] J.-P. Blaizot and E. Iancu, Phys. Rep. **359**, 355 (2002).
[25] Q. Wang, K. Redlich, H. Stöcker, and W. Greiner, Phys. Rev. Lett. **88**, 132303 (2002).
[26] A. Vilenkin, Phys. Rev. D **22**, 3080 (1980).
[27] D. E. Kharzeev, L. D. McLerran, and H. J. Warringa, Nucl. Phys. A **803**, 227 (2008).
[28] K. Fukushima, D. E. Kharzeev, and H. J. Warringa, Phys. Rev. D **78**, 074033 (2008).
[29] D. E. Kharzeev, J. Liao, S. A. Voloshin, and G. Wang, Prog. Part. Nucl. Phys. **88**, 1 (2016).
[30] D. Kharzeev, K. Landsteiner, A. Schmitt, and H.-U. Yee, Lect. Notes Phys. **871**, 1 (2013).
[31] X.-G. Huang, Rept. Prog. Phys. **79**, 076302 (2016).
[32] A. Vilenkin, Phys. Lett. B **80**, 150 (1978).
[33] J. Erdmenger, M. Haack, M. Kaminski, and A. Yarom, J. High Energy Phys. 01 (2009) 055.
[34] N. Banerjee, J. Bhattacharya, S. Bhattacharyya, S. Dutta, R. Loganayagam, and P. Surowka, J. High Energy Phys. 01 (2011) 094.
[35] D. T. Son and P. Surowka, Phys. Rev. Lett. **103**, 191601 (2009).
[36] J.-H. Gao, Z.-T. Liang, S. Pu, Q. Wang, and X.-N. Wang, Phys. Rev. Lett. **109**, 232301 (2012).
[37] D.-F. Hou, H. Liu, and H.-C. Ren, Phys. Rev. D **86**, 121703(R) (2012).
[38] J.-W. Chen, S. Pu, Q. Wang, and X.-N. Wang, Phys. Rev. Lett. **110**, 262301 (2013).
[39] J.-h. Gao and Q. Wang, Phys. Lett. B **749**, 542 (2015).
[40] Y. Hidaka, S. Pu, and D.-L. Yang, Phys. Rev. D **95**, 091901(R) (2017).
[41] J.-h. Gao, S. Pu, and Q. Wang, Phys. Rev. D **96**, 016002 (2017).
[42] J.-H. Gao, Z.-T. Liang, Q. Wang, and X.-N. Wang, Phys. Rev. D **98**, 036019 (2018).
[43] A. Huang, S. Shi, Y. Jiang, J. Liao, and P. Zhuang, Phys. Rev. D **98**, 036010 (2018).
[44] J.-h. Gao, J.-y. Pang, and Q. Wang, Phys. Rev. D **100**, 016008 (2019).
[45] R.-h. Fang, L.-g. Pang, Q. Wang, and X.-n. Wang, Phys. Rev. C **94**, 024904 (2016).
[46] N. Weickgenannt, X.-L. Sheng, E. Speranza, Q. Wang, and D. H. Rischke, Phys. Rev. D **100**, 056018 (2019).
[47] J.-H. Gao and Z.-T. Liang, Phys. Rev. D **100**, 056021 (2019).

[48] K. Hattori, Y. Hidaka, and D.-L. Yang, Phys. Rev. D **100**, 096011 (2019).
[49] M. Baznat, K. Gudima, A. Sorin, and O. Teryaev, Phys. Rev. C **88**, 061901(R) (2013).
[50] L. P. Csernai, V. K. Magas, and D. J. Wang, Phys. Rev. C **87**, 034906 (2013).
[51] L. P. Csernai, D. J. Wang, M. Bleicher, and H. Stöcker, Phys. Rev. C **90**, 021904(R) (2014).
[52] O. Teryaev and R. Usubov, Phys. Rev. C **92**, 014906 (2015).
[53] Y. Jiang, Z.-W. Lin, and J. Liao, Phys. Rev. C **94**, 044910 (2016).
[54] W.-T. Deng and X.-G. Huang, Phys. Rev. C **93**, 064907 (2016).
[55] Yu. B. Ivanov and A. A. Soldatov, Phys. Rev. C **95**, 054915 (2017).
[56] I. Karpenko and F. Becattini, Eur. Phys. J. C **77**, 213 (2017).
[57] Y. Xie, D. Wang, and L. P. Csernai, Phys. Rev. C **95**, 031901(R) (2017).
[58] H. Li, L.-G. Pang, Q. Wang, and X.-L. Xia Phys. Rev. C **96**, 054908 (2017).
[59] Y. Sun and C. M. Ko Phys. Rev. C **96**, 024906 (2017).
[60] F. Becattini and I. Karpenko, Phys. Rev. Lett. **120**, 012302 (2018).
[61] X.-L. Xia, H. Li, Z.-B. Tang, and Q. Wang, Phys. Rev. C **98**, 024905 (2018).
[62] H.-Z. Wu, L.-G. Pang, X.-G. Huang, and Q. Wang, Phys. Rev. Res. **1**, 033058 (2019).
[63] W. Florkowski, A. Kumar, R. Ryblewski, and A. Mazeliauskas, arXiv:1904.00002.
[64] Y. Sun and C. M. Ko, Phys. Rev. C **99**, 011903(R) (2019).
[65] D. Montenegro and G. Torrieri, Phys. Rev. D **100**, 056011 (2019).
[66] M. E. Peskin and D. V. Schroeder, *An Introduction to Quantum Field Theory* (Addison-Wesley, Reading, MA, 1995).
[67] R. Mertig, M. Bohm, and A. Denner, Comput. Phys. Commun. **64**, 345 (1991).
[68] V. Shtabovenko, R. Mertig, and F. Orellana, Comput. Phys. Commun. **207**, 432 (2016).
[69] H.-z. Wu, J. Zhang, L.-g. Pang, and Q. Wang, Comput. Phys. Commun. 106962 (2019).